

1 ~~Disappearing day-of-week ozone patterns in US nonattainment areas~~

2 Revisiting Day-of-Week Ozone Patterns in an Era of Evolving U.S.
3 Air Quality

4 Heather Simon¹, Christian Hogrefe², Andrew Whitehill², Kristen M. Foley², Jennifer Liljegren³,
5 Norm Possiel¹, Benjamin Wells¹, Barron H. Henderson¹, Lukas C. Valin², Gail Tonnesen⁴, K.
6 Wyatt Appel², Shannon Koplitz¹

7
8 ¹US Environmental Protection Agency, Office of Air and Radiation, Research Triangle Park, NC

9 ²US Environmental Protection Agency, Office of Research and Development, Research Triangle Park, NC

10 ³US Environmental Protection Agency, Region 5, Chicago, IL

11 ⁴US Environmental Protection Agency, Region 8, Denver, CO

12 *Correspondence to:* Heather Simon (Simon.Heather@epa.gov)

13
14 **Abstract.** Past work has shown that traffic patterns in the US and resulting NO_x emissions vary by day of week, with
15 NO_x emissions typically higher on weekdays than weekends. This pattern of emissions leads to different levels of
16 ozone on weekends versus weekdays and can be leveraged to understand how local ozone formation changes in
17 response to NO_x emissions perturbations in different urban areas. Specifically, areas with lower NO_x but higher ozone
18 on the weekends (the weekend effect) can be characterized as NO_x-saturated and areas with both lower NO_x and
19 ozone on weekends (the weekday effect) can be characterized as NO_x-limited. In this analysis we assess maximum
20 daily 8-hr average (MDA8) ozone weekend-weekday differences across 51 US nonattainment areas using 18 years of
21 observed and modeled data from 2002-2019 using two metrics: mean MDA8 ozone and percentage of days with
22 MDA8 ozone > 70 ppb. In addition, we quantify the modeled and observed trends in these weekend-weekday
23 differences across this period of substantial NO_x emissions reductions in the US. The model assessment is carried out
24 using EPA's Air QUALity Time Series Project (EQUATES) CMAQ dataset. We identify 3 types of MDA8 ozone
25 trends ~~occurring~~occurring across the US: ~~disappearing weekend effect~~transitioning chemical regime, disappearing
26 weekday effect, and no trend. The ~~disappearing weekend effect~~transitioning chemical regime trend occurs in a subset
27 of large urban areas that were NO_x-saturated (i.e., VOC-limited) at the beginning of the analysis period but
28 transitioned to mixed chemical regimes or NO_x-limited conditions by the end of the analysis period. Nine areas have
29 ~~disappearing weekend effect~~strong transitioning chemical regime trends ~~in~~using both ~~datasets~~modeled and observed
30 data and with both metrics indicating strong agreement that they are shifting to more NO_x-limited conditions:
31 Milwaukee, Houston, Phoenix, Denver, Northern Wasatch Front, Southern Wasatch Front, Las Vegas, Los Angeles –
32 San Bernardino County, Los Angeles – South Coast, and San Diego. The disappearing weekday effect was identified
33 for multiple rural and agricultural areas of California which were NO_x-limited for the entire analysis period but appear
34 to become less influenced by local day of week emission patterns in more recent years. Finally, we discuss a variety
35 of reasons why there are no ~~statistically significant~~ trends in certain areas including complex impacts of heterogeneous
36 source mixes and stochastic impacts of meteorology. Overall, this assessment finds that the EQUATES modeling
37 simulations indicate more NO_x-saturated conditions than the observations but do a good job of capturing year-to-year
38 changes in weekend-weekday MDA8 ozone patterns.

40 **1 Introduction**

41 Ground-level ozone (O₃), a key component of photochemical smog, has adverse impacts on human health and
42 ecosystems (U.S. Environmental Protection Agency, 2019). In the United States (US), the Clean Air Act Amendments
43 of 1970 instruct the Environmental Protection Agency (EPA) to set National Ambient Air Quality Standards
44 (NAAQS) for criteria pollutants. Since 1979, O₃ has served as the indicator species for the criteria pollutant of
45 photochemical oxidants (44 FR 8202) and since 1997, the form of the standard has been determined by the 3-year
46 average of the annual 4th-highest daily maximum 8-hour concentration (MDA8) (62 FR 38856). In 2015, the O₃
47 NAAQS were revised to the current level of 0.070 ppm or 70 ppb (80 FR 65291). As of 2018, 52 areas in the US had
48 been designated as nonattainment of the 2015 O₃ NAAQS (83 FR 25776; 83 FR 35136; 83 FR 52157).

49
50 O₃ is predominantly a secondary pollutant formed from photochemical reactions of nitrogen oxides (NO_x) and volatile
51 organic compounds (VOCs). Ground-level O₃ concentrations are a complex nonlinear function of the chemistry of
52 natural and anthropogenic precursor emissions, as well as meteorology, transport, and deposition (Seinfeld and Pandis,
53 2016). O₃ formation rates depend on the concentrations and speciation of NO_x and VOCs. To reduce ambient O₃
54 concentrations, control strategies have been enacted in the US over the last 50 years to ~~control~~ reduce the emissions of
55 both NO_x and VOCs (Simon et al., 2015).

56
57 The effectiveness of different control strategies on O₃ production rates depends on the photochemical environment
58 under which ozone is formed. Ozone formation environments are typically categorized as either NO_x-limited or NO_x-
59 saturated, with a mixed or transitional regime between the two (Sillman, 1995, 1999; Sillman et al., 1990). In the NO_x-
60 limited regime, ambient ozone concentrations will respond more strongly to changes in NO_x emissions than VOC
61 emissions. In contrast, in a NO_x-saturated (or VOC-limited) regime, ozone will increase with NO_x emission controls
62 but will decrease with VOC emissions controls. Understanding the photochemical regimes of different ozone
63 nonattainment areas and how they have changed over time is important for understanding the impacts of previous
64 control strategies and guiding future control strategies to have the maximum health benefit with the least economic
65 burden.

66
67 Different methods have been proposed to determine ozone formation regimes and their changes over time. One
68 common method used to evaluate ozone formation chemistry is through day-of-week (DOW) differences in the
69 concentration of ozone and its precursors. The DOW effects leverage NO_x emissions differences between weekdays
70 and weekends (Marr and Harley, 2002a, b). In the US, onroad vehicles are a dominant source of NO_x emissions (Toro
71 et al., 2021). Diesel vehicle traffic tends to be higher on weekdays (Monday through Friday) than on weekends
72 (Saturday and Sunday). This results in higher NO_x emissions on weekdays than weekends (Marr and Harley, 2002a,
73 b). Daily varying emissions sources such as diesel vehicles are not a major source of VOC emissions. In addition,
74 VOC emissions in some areas are dominated by biogenic emissions that do not vary by day of week. Consequently,
75 VOC emissions are generally similar on weekends and weekdays in most areas. The result of DOW NO_x patterns is
76 that ozone concentrations tend to be higher on weekends than weekdays in NO_x-saturated areas and lower on
77 weekends than weekdays in NO_x-limited areas (Kopplitz et al., 2022). DOW differences in ozone were first reported

78 in the 1970s (Bruntz et al., 1974; Cleveland et al., 1974). In 2002 the DOW ozone differences in California were
79 explicitly tied to DOW patterns in diesel vehicle traffic (Marr and Harley, 2002a, b). Since that time, multiple studies
80 have used DOW ozone patterns to assess ozone chemical formation regimes in individual US cities including Los
81 Angeles, California (Chinkin et al., 2003; Fujita et al., 2003b; Fujita et al., 2003a; Gao, 2007; Gao and Niemeier,
82 2007; Warneke et al., 2013), Fresno, California (De Foy et al., 2020), Sacramento, California (Murphy et al., 2007),
83 Phoenix, Arizona (Atkinson-Palombo et al., 2006), Atlanta, Georgia (Blanchard and Tanenbaum, 2006), Baltimore,
84 Maryland (Roberts et al., 2022), and New York City, New York (Singh and Kavouras, 2022). A smaller number of
85 studies have assessed ozone DOW patterns across multiple US urban areas (Blanchard et al., 2008; Jaffe et al., 2022;
86 Koo et al., 2012; Koplitz et al., 2022; Pun et al., 2003). Additionally, ozone DOW patterns have been used as a method
87 for assessing chemical formation regimes outside of the US in Shanghai, China (Zhang et al., 2023), the Lesser Antilles
88 Archipelago (Plocoste et al., 2018), Rio de Janeiro, Brazil (Martins et al., 2015), Santiago, Chile (Rubio et al., 2011),
89 Andalusia, Spain (Adame et al., 2014), the Iberian Peninsula (Jiménez et al., 2005), Athens, Greece (Paschalidou and
90 Kassomenos, 2004) and in multiple other European cities (Pires, 2012). One complication with interpreting DOW O₃
91 patterns is that O₃ concentrations in urban areas are generally impacted by a mix of transport and local formation. O₃
92 transport can occur over a variety of timescales. In some locations there could be a regional O₃ DOW effect that might
93 be evident as a slightly lagged timescale depending on typical transport times from major upwind urban source areas.

94
95 Previous work has shown a substantial decrease in NO_x emissions in the US over the past 20 years as a result of
96 national, state, and local regulations (Krotkov et al., 2016; Lamsal et al., 2015; Russell et al., 2012; Toro et al., 2021).
97 Concurrent with the US NO_x decreases, multiple studies have found that ozone chemical formation regimes have also
98 changed in the US (Jin et al., 2020; Jin et al., 2017; Koplitz et al., 2022). In this paper, we focus on 51 areas in the US
99 which were designated in 2018 as nonattainment ([https://www.epa.gov/green-book/green-book-8-hour-ozone-2015-](https://www.epa.gov/green-book/green-book-8-hour-ozone-2015-area-information)
100 [area-information](https://www.epa.gov/green-book/green-book-8-hour-ozone-2015-area-information)) under the 2015 O₃ NAAQS (some of these areas have since been redesignated to attainment based
101 on clean monitoring data). We look at changes in DOW patterns in the US over 18 years from 2002 to 2019 using
102 both measured and modeled data to provide insights into how ozone formation chemistry has changed in the US as a
103 result of emissions reductions, and to assess how well modeling is able to capture the observed changes. This 18-year
104 dataset, which is part of EPA's Air Quality Time Series Project (EQUATES), is unique in its application of consistent
105 emissions and modeling methodologies across the entire analysis period providing an opportunity to assess multi-year
106 trends.

107

108 **2 Methods**

109

110 For this assessment we use MDA8 ozone monitoring data obtained from EPA's Air Quality System (AQS)
111 (<https://www.epa.gov/aqs>) and MDA8 ozone modeling data from simulations of the Community Multiscale Air
112 Quality model version 5.3.2 (CMAQv5.3.2). The CMAQ model data are part of EQUATES which provides an 18-
113 year set of modeled meteorology, emissions, air quality and pollutant deposition spanning the years 2002 through
114 2019 using consistent modeling methods across years. The CMAQv5.3.2 model configuration, including input data,

115 boundary conditions, and science options are available from US EPA (EpaEPA, 2021). The emissions inventories
116 developed for the EQUATES CMAQ modeling are described in (Foley et al., 2023).

117
118 We extract CMAQ modeling data only for days and grid-cells with monitoring data such that both datasets are paired
119 in time and location. Both datasets are subset to ozone monitors located within 51 of the 52 areas that were designated
120 in 2018 as nonattainment for the 2015 O₃ NAAQS (a list of areas is available in Tables S1 and S2) (83 FR 25776; 83
121 FR 35136; 83 FR 52157). Because this analysis focuses on May-September data, we do not include data from the
122 Uintah Basin nonattainment area for which violations of the NAAQS predominantly occur in winter months. Data are
123 analyzed for the 18-year period of the EQUATES modeling dataset.

124
125 We start by analyzing changes in MDA8 ozone between weekends and weekdays pooled across all monitoring
126 locations for each nonattainment area for 5-year rolling periods (i.e., 14 different periods covering the 18-year
127 timeseries). We pool data into 5-year periods for several reasons. First, it dampens impacts of interannual meteorology
128 that can contribute to large year-to-year changes in ozone for a given location. Previous work has shown that
129 differential meteorological patterns on weekends versus weekdays impacts ozone DOW patterns in a single year and
130 that pooling data across multiple years can reduce this effect (Pierce et al., 2010). Second, it provides a larger sample
131 size for calculating ozone differences between weekends and weekdays. The use of 5-year periods does, however,
132 limit this analysis' ability to parse out changes in weekend-weekday differences that have occurred due to emissions
133 changes in the most recent individual years analyzed. For example, any changes occurring only in 2018 and/or 2019
134 would be dampened in the 2015-2019 pooled data.

135
136 For the purpose of quantifying differences in weekend versus weekday O₃ concentrations, we use Sundays to represent
137 weekends (WE) and Tuesdays, Wednesdays and Thursdays to represent weekdays (WD). We do not include ozone
138 on Monday and Saturday to minimize any carryover impacts on concentrations from the previous day and we exclude
139 Friday as it may exhibit somewhat different emissions patterns than the other weekdays.

140
141 We use two metrics to quantify differences in MDA8 ozone between weekends and weekdays. First, we quantify mean
142 differences in MDA8 ozone across the entire distribution of days in each season (Winter = Dec, Jan, Feb; Spring =
143 Mar, Apr, May, Summer = Jun, Jul, Aug, Fall = Sep, Oct, Nov, ozone season = May-Sep) using Eq. (1), where O_{3,WE}
144 represents MDA8 O₃ on Sundays and O_{3,WD} represents MDA8 O₃ on Tuesdays, Wednesdays, and Thursdays.

$$145 \Delta \overline{O_{3,DOW}} = \overline{O_{3,WE}} - \overline{O_{3,WD}} \quad (1)$$

146
147
148 In this study we mainly focus on differences during the May-Sep ozone season. The Welch's t-test (Welch, 1947) is
149 used to denote whether the mean WE-WD difference is statistically different from zero (p < 0.05). Within each
150 nonattainment area, the t-test calculation was used to compare the means of every weekday and every weekend day
151 in a 5-year window, treating each day as an independent observation. All available ozone monitoring data and model

152 output from all monitoring locations within each nonattainment area are included in the calculation, providing a
153 measure of average behavior across each area. We also examine 24-hour average modeled formaldehyde and NO_x
154 concentrations at each of the ozone monitor locations to verify whether the model shows expected patterns of higher
155 NO_x on weekdays than on weekends and trends in these ozone precursors. Formaldehyde is used as an indicator of
156 first-generation VOC reaction products for this purpose. We note that monitoring data for VOCs and NO_x are much
157 sparser in terms of sampling frequency and spatial density than ozone measurements, so we rely on the model alone
158 to verify underlying day-of-week patterns in precursor compounds.

159
160 Second, similar to (Jaffe et al., 2022), we look at the percent of days with MDA8 ozone values above the NAAQS
161 level of 70 ppb. We calculate the percent of total weekends and weekdays in May-Sep for which MDA8 ozone
162 concentrations exceeded 70 ppb as shown in Eq. (2).

$$163 \Delta O_{3,DOW,\%>70} = O_{3,WE,\%>70} - O_{3,WD,\%>70} \quad (2)$$

164
165
166 For this calculation, a day is characterized as exceeding the NAAQS in an area if measured and/or modeled MDA8
167 ozone is above 70 ppb at the location of any ozone monitor within the area. In this way we are tracking days where
168 some portion of the area has observed or modeled MDA8 ozone above 70 ppb, but the analysis does not distinguish
169 whether the high ozone concentrations are localized over a small portion of the area or widespread across multiple
170 monitoring locations. This analysis also does not consider whether days with modeled MDA8 ozone above 70 ppb
171 occur simultaneously with observed MDA8 ozone above 70 ppb. We use the Fisher's exact test (Fisher, 1935; Mehta
172 and Patel, 1983) to determine whether the proportion of days above 70 ppb differs significantly (p < 0.05) between
173 weekends and weekdays.

174
175 Next, we use the Theil-Sen estimator (Sen, 1968; Theil, 1992) to determine the multi-year trends in $\overline{\Delta O_{3,DOW}}$ and
176 $\Delta O_{3,DOW,\%>70}$ for each area. This nonparametric approach was chosen due to the small sample size (n=14 5-year
177 windows) and the fact that the ~~Theil~~Theil-Sen estimator does not require any assumptions on the distribution of the
178 residuals. The Mann-Kendall test (Kendall, 1975; Mann, 1945) is used to determine the statistical significance of the
179 derived trends in WE-WD O₃ differences. ~~For each derived trend, we also document the 95% confidence~~
180 ~~interval~~MDA8 O₃ differences. ~~For each derived trend, we also document the 95% confidence interval. Because we~~
181 ~~use a 5-year rolling window for each area, the individual data points in the trends analysis are correlated. While this~~
182 ~~should not systematically bias the calculated slopes, it will lead to lower P-values and narrower 95% confidence~~
183 ~~intervals than would be calculated if the data points were uncorrelated. However, the P-value is still informative to~~
184 ~~characterize which areas have the strongest trends. Therefore, while we do report P-values we do not rely on a strict~~
185 ~~threshold for determining statistical significance.~~

186
187 Finally, investigation of relationships between WE-WD MDA8 O₃ and meteorological parameters used the
188 meteorological dataset developed by and described in (Wells et al., 2021). Meteorological parameters were similarly

189 [compared across weekends and weekdays, matching times and locations of the ozone analysis and using the same](#)
190 [statistical methods for comparison.](#)

191

192 **3 Results**

193

194 **3.1 Modeled NO_x and formaldehyde day-of-week patterns**

195

196 [For all but one of the 51 areas, the model shows clear patterns of higher NO_x concentrations on weekdays than](#)
197 [weekends. We first look at modeled NO_x and formaldehyde day-of-week patterns to better understand how daily](#)
198 [changes in precursor emissions impact modeled day-of-week ozone patterns. We chose to focus on modeled data here](#)
199 [because of the ubiquitous spatial and temporal coverage provided in the model for these pollutants allowing us to](#)
200 [evaluate these pollutants on the same days and at the same locations as the ozone monitors. We note that some](#)
201 [observed NO_x data can also be used for this purpose, although NO_x data are not available for all nonattainment areas](#)
202 [and are not available at the locations of all ozone monitors even within nonattainment areas with NO_x monitoring data.](#)
203 [A comparison of monitored and observed trends in NO_x day-of-week differences provided in Figures S-1 through S-](#)
204 [26 shows that the model does reasonably well at capturing the patterns in the limited observational dataset that is](#)
205 [available. Due to the sparsity of formaldehyde measurements, both spatially and temporally \(formaldehyde is](#)
206 [commonly measured at a 1-in-6 day or 1-in-12 day frequency\), a similar comparison cannot be made for modeled and](#)
207 [measured formaldehyde. However, with more recent requirements for formaldehyde measurements at Photochemical](#)
208 [Assessment Monitoring Stations \(PAMS\) locations starting in the 2017-2019 time-period, future assessments may](#)
209 [have additional measured formaldehyde data that could be used for this purpose.](#)

210

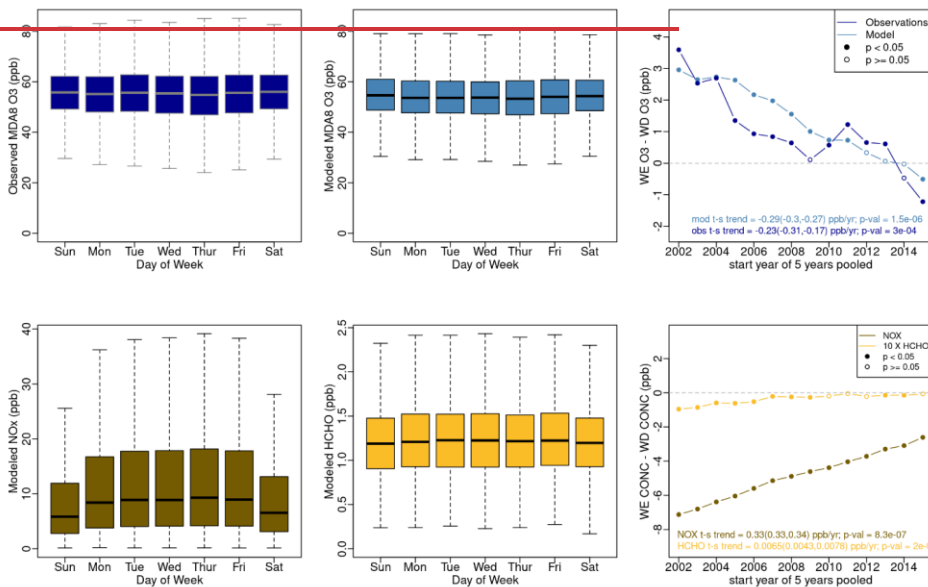
211 [Utilizing the complete model data set, we see clear patterns of higher NO_x concentrations on weekdays than weekends](#)
212 [for all but one of the 51 areas and relatively constant formaldehyde concentrations across May-Sep days for the entire](#)
213 [2002-2019 analysis period. This is consistent with the underlying assumption in the ozone day-of-week analyses](#)
214 [discussed above. Here we describe examples of the modeled NO_x and formaldehyde day of week patterns using the](#)
215 [data for Denver, CO and Los Angeles, CA to show typical patterns in large urban areas and Butte County, CA to show](#)
216 [a typical pattern in a more rural area in Figures 1, 2, and 3, respectively. The modeled WE-WD differences in NO_x](#)
217 [concentrations are more pronounced in large urban areas such as Los Angeles and Denver than in rural or agricultural](#)
218 [areas such as Butte County. The only area that does not demonstrate higher modeled NO_x concentrations on weekdays](#)
219 [than weekends is Door County, WI \(Figure S-127\). Higher NO_x emissions on weekdays are typically associated with](#)
220 [commuting patterns and greater vehicular activity from commercial truck traffic. The nonattainment portion of Door](#)
221 [County, which was fully redesignated to attainment in 2022 \(87 FR 25410\), is located at the tip of a peninsula on Lake](#)
222 [Michigan and a rural recreation and tourist destination \(i.e., likely to see more weekend activity\). Consequently, the](#)
223 [area does not follow typical weekday-weekend emission patterns and therefore modeled NO_x concentration patterns](#)
224 [are unlike those of other areas. While the model does not predict substantial day-of-week formaldehyde differences](#)

225 in most areas, there are small modeled weekday-formaldehyde enhancements on weekdays compared to weekends in
 226 some areas such as Chicago (Figure S-228).

227
 228 Theil-Sen trends show that differences in modeled WE versus WD NO_x have diminished significantly over time in
 229 most areas (e.g. Figures 1, 2 and 3). The modeled WE versus WD differences in formaldehyde are also diminishing
 230 over time but to a much lesser extent. As total emissions have decreased, absolute modeled and observed
 231 concentrations of NO_x have also decreased: along with the WE-WD differences in NO_x. Figures S-533 and S-634
 232 show that the modeled WE versus WD NO_x trends remain significant whether tracking absolute or normalized NO_x
 233 differences in Denver and Los Angeles, which is consistent with modeled WE-WD NO_x trends seen in all but ten of
 234 the nonattainment areas. In nine of these areas (Houston, TX; Las Vegas, NV; Muskegon, MI; New York, NY;
 235 Phoenix, AZ; San Diego, CA; St. Louis, MO-IL; Tuolumne County, CA; and Yuma, AZ) while absolute modeled
 236 WE-WD NO_x differences have diminished significantly substantially but there is no significant trend little change in
 237 relative WE-WD differences. In Mariposa County, CA neither absolute nor relative WE-WD NO_x differences have
 238 significant trends from 2002-2019; changed substantially between 2002-2019. These findings that NO_x concentrations
 239 and NO_x day-of-week patterns have decreased over time is consistent with national trends reported by (Jaffe et al.,
 240 2022).

241

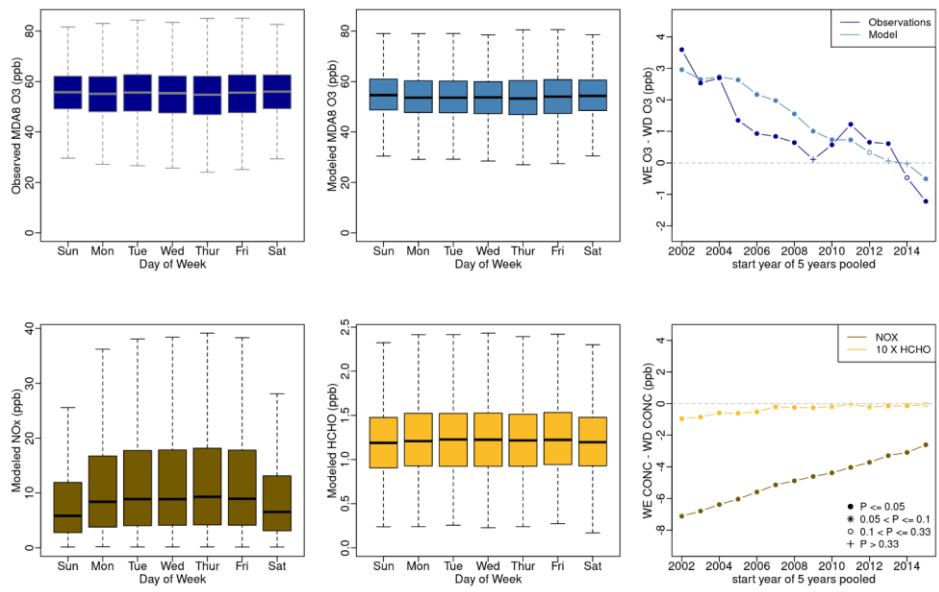
Denver Metro/North Front Range, CO



242

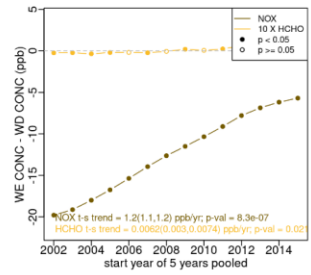
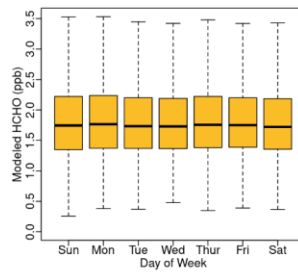
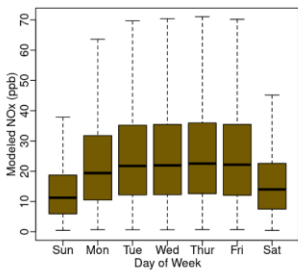
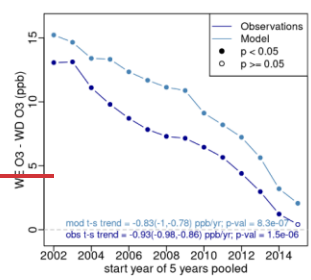
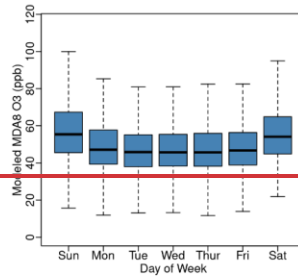
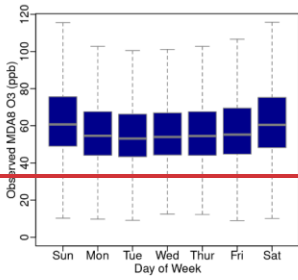
243

Denver Metro/North Front Range, CO



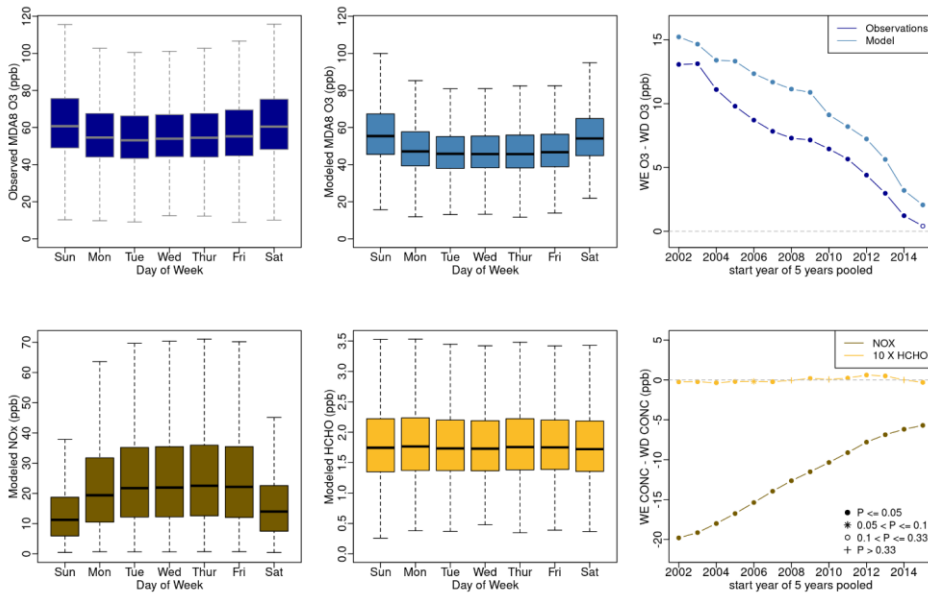
244
 245 **Figure 1. Denver area 2002-2019 May-Sep: observed (top left) and modeled (top center) MDA8 ozone distribution by day**
 246 **of week; modeled NO_x (bottom left) and modeled formaldehyde (bottom center) distribution by day of week; observed and**
 247 **modeled trends in $\Delta\bar{O}_{3,DOW}$ (top right); modeled trends in WE-WD NO_x and formaldehyde differences (bottom right). The**
 248 **distributions by day of the week are for the entire 18 years with each box representing the 25th to 75th percentile for that**
 249 **day of the week across all 18 years, the whiskers representing the 1.5 times the interquartile range, and the bold line inside**
 250 **the box representing the median. WE-WD differences (top and bottom right) are based on 5-year rolling periods. P-values**
 251 **denoted by symbols in the right-hand panels refer to the t-test results comparing mean weekend and weekday values for**
 252 **each 5-year period.**

Los Angeles-South Coast Air Basin, CA



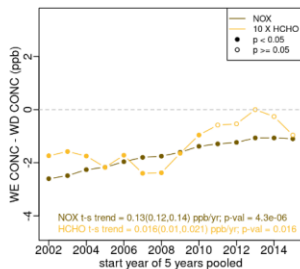
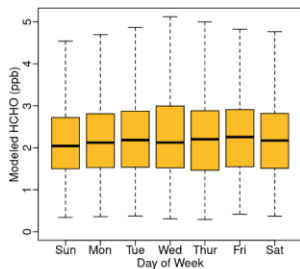
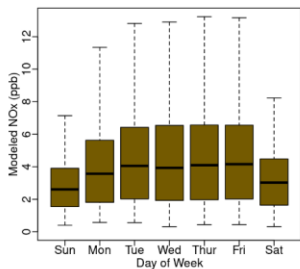
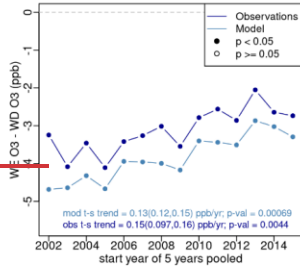
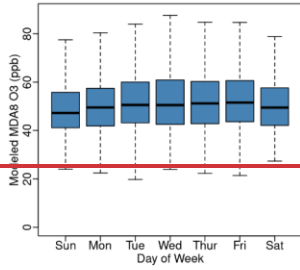
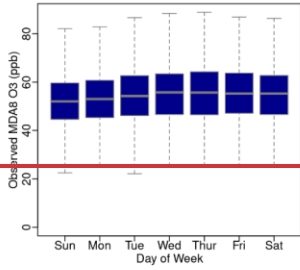
253
254

Los Angeles-South Coast Air Basin, CA

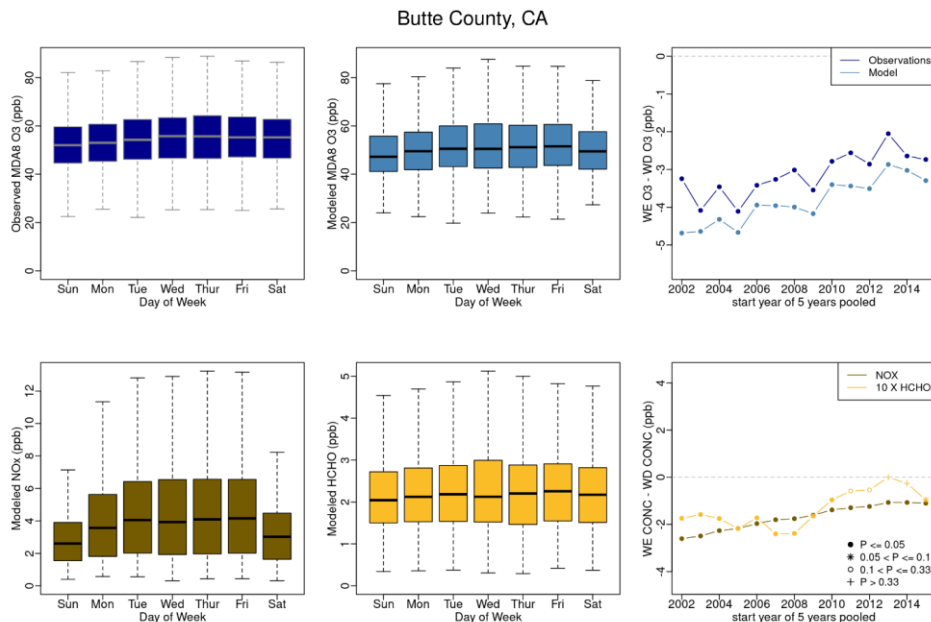


255
 256 **Figure 2. Los Angeles area 2002-2019 May-Sep: observed (top left) and modeled (top center) MDA8 ozone distribution by**
 257 **day of week; modeled NO_x (bottom left) and modeled formaldehyde (bottom center) distribution by day of week; observed**
 258 **and modeled trends in $\Delta\bar{O}_{3,DOW}$ (top right); modeled trends in WE-WD NO_x and formaldehyde differences (bottom right).**
 259 **The distributions by day of the week are for the entire 18 years with each box representing the 25th to 75th percentile for**
 260 **that day of the week across all 18 years, the whiskers representing the 1.5 times the interquartile range, and the bold line**
 261 **inside the box representing the median. WE-WD differences (top and bottom right) are based on 5-year rolling periods. P-**
 262 **values denoted by symbols in the right-hand panels refer to the t-test results comparing mean weekend and weekday values**
 263 **for each 5-year period.**

Butte County, CA



264
265

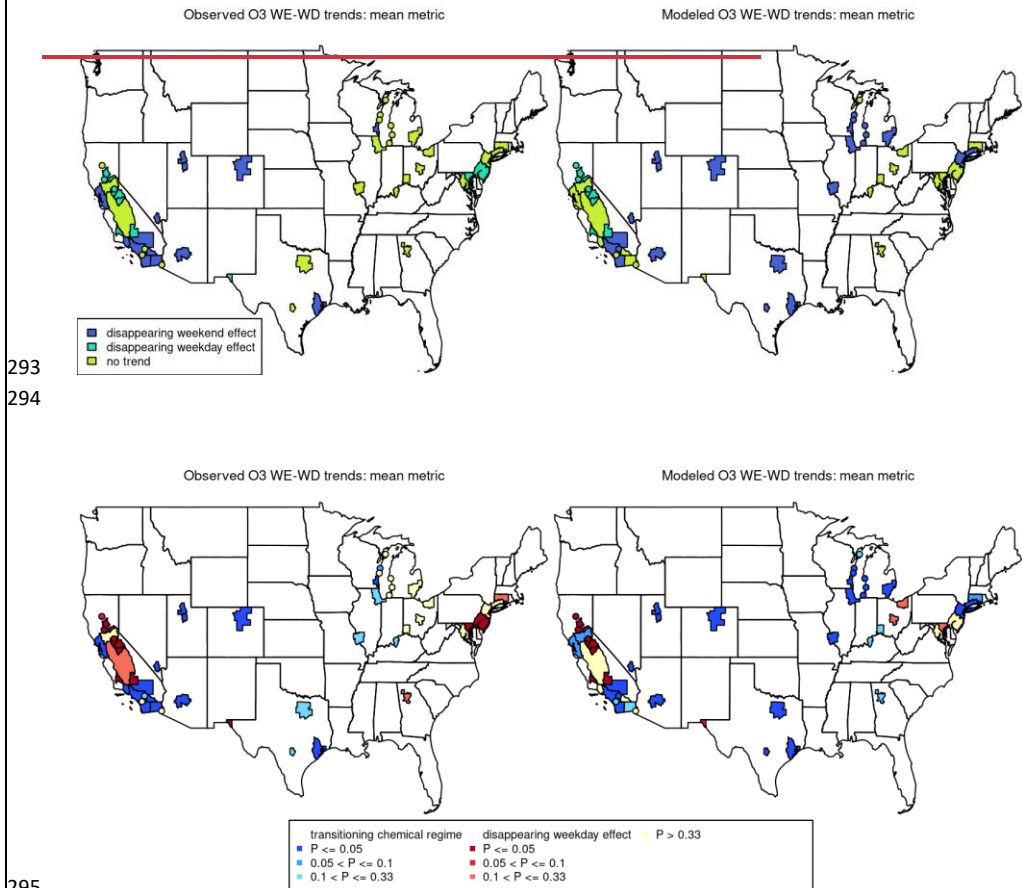


266
 267 **Figure 3. Butte County, CA area 2002-2019 May-Sep: observed (top left) and modeled (top center) MDA8 ozone distribution**
 268 **by day of week; modeled NO_x (bottom left) and modeled formaldehyde (bottom center) distribution by day of week;**
 269 **observed and modeled trends in $\Delta\bar{O}_{3,DOW}$ (top right); modeled trends in WE-WD NO_x and formaldehyde**
 270 **differences (bottom right). The distributions by day of the week are for the entire 18 years with each box representing the 25th to 75th**
 271 **percentile for that day of the week across all 18 years, the whiskers representing the 1.5 times the interquartile range, and the bold line inside the box representing the median. WE-WD differences (top and bottom right) are based on 5-year rolling**
 272 **periods. P-values denoted by symbols in the right-hand panels refer to the t-test results comparing mean weekend and**
 273 **weekday values for each 5-year period.**
 274
 275

276 **3.2 Trend types of ozone day-of-week patterns**
 277

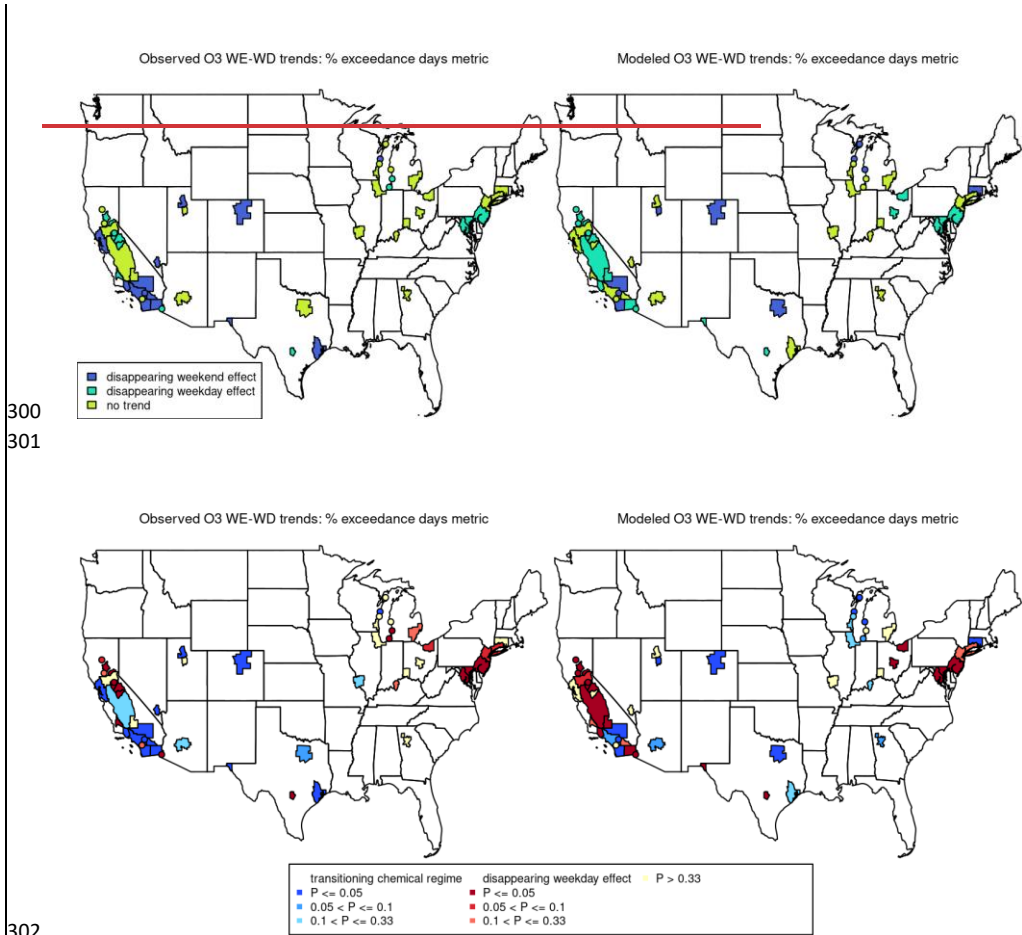
278 Within any 5-year window, NO_x-saturated areas display a “weekend effect” meaning that MDA8 ozone
 279 concentrations were ~~statistically~~ higher on weekends than on weekdays and NO_x-limited areas display a “weekday
 280 effect” meaning that ozone concentrations were ~~statistically~~ higher on weekdays than on weekends. We categorize the
 281 trends in MDA8 ozone DOW patterns into 3 discrete categories: 1) ~~disappearing weekend effect~~transitioning chemical
 282 regime (i.e. areas that went from NO_x-saturated to NO_x-limited), 2) disappearing weekday effect (i.e. areas that went
 283 from NO_x-limited to approaching zero in terms of DOW differences), and 3) areas with no ~~significant change~~trend
 284 over the 18-year time period. ~~Disappearing weekend effect~~Transitioning chemical regime areas are characterized by
 285 a negative ~~ThielTheil~~-Sen slope (e.g. Denver and Los Angeles in Figures 1 and 2 respectively). Disappearing weekday
 286 effect areas are characterized by a positive ~~ThielTheil~~-Sen slope (e.g. Butte County in Figure 3). Areas with no trend
 287 are characterized by ~~a lack of significance~~, P-values > 0.33 as determined by the Mann-Kendall test. Trend types for
 288 all 51 areas based on observed and modeled datasets are shown in Figure 4 and 5. Areas are color-coded by P-value
 289 ranges for both the transitional chemical regime trend type and the disappearing weekday effect trend type. Given the

290 autocorrelation of the timeseries data we do not apply any strict P-value thresholds for identifying these trend types
 291 but we do note that areas with lower P-values show stronger trends than those with higher P-values.
 292



293
 294

295
 296 **Figure 4.** Map of ozone nonattainment areas color coded by trends in mean **MDAS** ozone day of week differences ($\Delta\bar{O}_{3,DOW}$)
 297 using observed data (left) and modeled data (right) over an 18-year period from 2002-2019. Ozone nonattainment areas less
 298 than 3000 km² in area are shown as dots on the map for visibility.
 299



300
301

302
303
304
305
306
307

Figure 5. Map of ozone nonattainment areas color coded by trends in ozone day of week differences based on the percentage of days with MDA8 ozone >70 ppb-MDA8 ($\Delta O_{3,DOW,\%}>70$) using observed data (left) and modeled data (right) over an 18-year period from 2002-2019. Ozone nonattainment areas less than 3000 km² in area are shown as dots on the map for visibility.

308
309

3.2.1 “Disappearing weekend effect/Transitioning chemical regime” case studies

310
311
312
313
314

The ~~disappearing weekend effect~~transitioning chemical regime trend is typical of areas that initially had strongly positive ozone WE-WD differences (i.e., mean MDA8 ozone is higher on weekends than on weekdays), suggesting NO_x-saturated conditions, at the beginning of the analysis period. These areas typically transition into ~~significant near-zero or~~ negative WE-WD MDA8 O₃ differences by the most recent 5-year window, suggesting a shift to NO_x-limited conditions by the end of the analysis period. Of the 51 nonattainment areas analyzed, ~~15 exhibit this type of trend~~

315 based on observed data and 23 based on modeled data for $\Delta\overline{O_{3,DOW}}$. 21 exhibit this type of trend for the $\Delta\overline{O_{3,DOW}}$
316 metric based on observed data (14 with P-Values < 0.05, 1 with a P-Value between 0.05 and 0.1 and 6 with P-Values
317 between 0.1 and 0.33) and 31 based on modeled data (22 with P-Values < 0.05, 3 with P-Values between 0.05 and 0.1
318 and 6 with P-Values between 0.1 and 0.33). Of the 51 nonattainment areas analyzed, 17 exhibit this type of trend for
319 the $\Delta O_{3,DOW,\%>70}$ metric based on observed data (14 with P-Values < 0.05 and 3 with P-Values between 0.1 and
320 0.33) and 19 based on modeled data (10 with P-Values < 0.05, 4 with P-Values between 0.05 and 0.1 and 5 with P-
321 Values between 0.1 and 0.33). This type of trend is consistent with previously reported national DOW trends reported
322 across major metropolitan areas using only the $\Delta O_{3,DOW,\%>70}$ metric (Jaffe et al., 2022).

323
324 Two areas that exhibit this trend for $\Delta\overline{O_{3,DOW}}$ are Denver and Los Angeles shown in Figures 1 and 2 respectively. In
325 Denver, the modeled and observed $\Delta\overline{O_{3,DOW}}$ are statistically significant and $\overline{O_{3,DOW}}$ was in the range of +3 to
326 +4 ppb at the beginning of the analysis period for Denver. Both the model and observed and model data have
327 statistically significant decreasing Theil-Sen slopes for $\Delta\overline{O_{3,DOW}}$, -0.29-23 (observed) and -0.29 (modeled) ppb/yr
328 and -0.23 ppb/yr for Denver and Los Angeles respectively, with P-Values less than 0.001. In the most recent 2015-
329 2019 5-year window, both modeled and observed $\Delta\overline{O_{3,DOW}}$ are negative and statistically different from zero,
330 suggesting a shift to NO_x-limited conditions. While the results shown in Figure 1 represent aggregated measured
331 MDA8 ozone data across all Denver nonattainment area monitors, Figure 6 shows behavior at three specific monitors
332 in Denver with monitoring records covering the majority of the analysis period. All three sites were located to the
333 south and southwest of the Denver urban area. The Welch monitor is located closer to the Denver urban area in
334 proximity to two major highways. While the monitored negative observed and modeled negative Theil-Sen slopes
335 for $\Delta\overline{O_{3,DOW}}$ holds $\overline{O_{3,DOW}}$ hold at all 3 sites, there are differences in the magnitude of the slopes and the sign of
336 $\Delta\overline{O_{3,DOW}}$ across sites. For instance, the Welch and Highland Reservoir sites both have statistically significant positive
337 $\Delta\overline{O_{3,DOW}}$ at the beginning of the analysis period suggesting both sites were NO_x-saturated in the early 2000s. While
338 the Chatfield site had positive $\Delta\overline{O_{3,DOW}}$ at the beginning of the analysis period, larger P-Values indicate the differences
339 were may not be statistically different from zero, suggesting that this location may have already been transitioning to
340 NO_x-limited conditions in the early-to-mid 2000s. The model predicts that all three sites have non-significant $\Delta\overline{O_{3,DOW}}$
341 that are negative $\Delta\overline{O_{3,DOW}}$ but close to zero at the end of the analysis period while observations show the substantial
342 negative $\Delta\overline{O_{3,DOW}}$ to be statistically significant $\overline{O_{3,DOW}}$ values at Chatfield and Highland Reservoir. This suggests that
343 the model may understate the NO_x-limited conditions in recent years at these locations. Los Angeles provides another
344 example of an area where both the model and the observations had strongly positive $\Delta\overline{O_{3,DOW}}$ at the beginning of the
345 analysis period (+13 to +15 ppb) and disappearing weekend effect/transitioning chemical regime trends (Figure 2)-
346 with observed and modeled Theil-Sen slopes of 0.93 and 0.83 ppb/yr. Similar to Denver, site to site differences in the
347 magnitude of $\Delta\overline{O_{3,DOW}}$ are evident in Los Angeles (Figure S-733) but the disappearing weekend effect/transitioning
348 chemical regime trend is fairly consistent across sites. Similar types of trends in Chicago and Houston are shown in
349 supplemental figures S-228 and S-329.

350

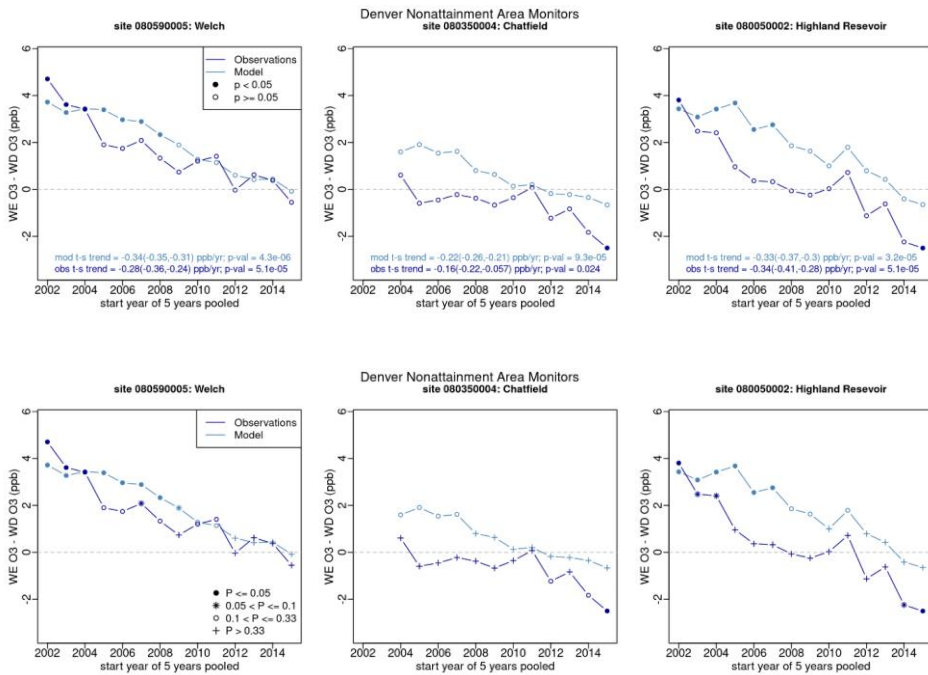
Formatted: English (United States)

Formatted: English (United States)

351 In general, similar disappearing weekend effect trends in $\Delta O_{3,DOW,\%>70}$ are evident, however this metric appears to be
 352 noisier perhaps because it is capturing the frequency of extreme events which have a more stochastic nature than mean
 353 ozone differences. Specifically, since there are a low number of exceedance days for most nonattainment areas in any
 354 given year, a metric based on the percentage of those days falling on a Sunday versus a Tuesday, Wednesday or
 355 Thursday will be inherently more noisy than a metric based on mean values. Figures 7 and 8 show $\Delta O_{3,DOW,\%>70}$
 356 Thiel-Sen trends for Denver and Los Angeles. In general, similar transitioning chemical regime trends in $\Delta O_{3,DOW,\%>70}$
 357 are evident in Denver and Los Angeles (Figures 7 and 8). In both cases, the model underpredicts both the percentage
 358 of days with MDA8 $O_3 > 70$ ppb and the Thiel-Sen slope. Additional examples of results for $\Delta O_{3,DOW,\%>70}$ are
 359 provided for Chicago, Houston and New York City in Figure S-935, S-4936 and S-4437 respectively.

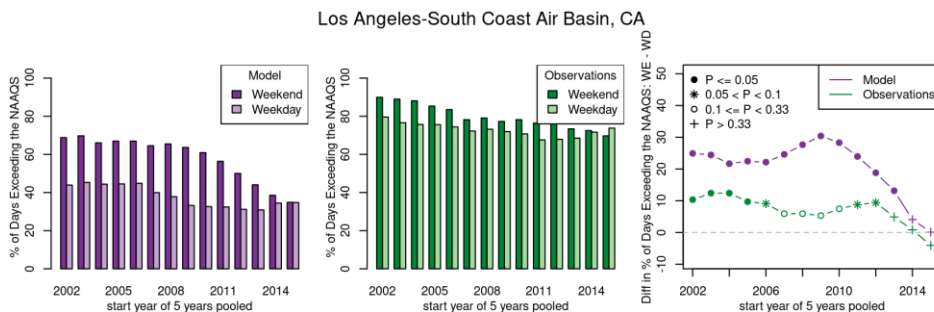
360
361

362
363



364
365
366
367
368

Figure 6. Observed and modeled May-Sep trends in mean MDA8 ozone day of week differences ($\Delta O_{3,DOW}$) at three Denver area monitoring locations for 2002-2019 plotted as 5-year rolling periods. P-values denoted by symbols refer to the t-test results comparing mean weekend and weekday values for each 5-year period.

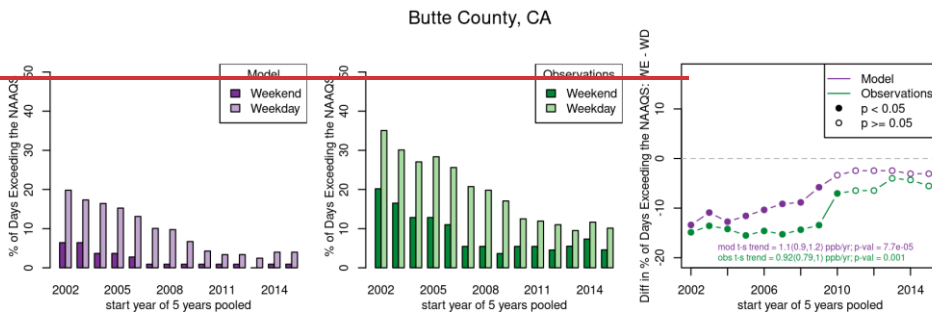


381
 382 **Figure 8. Modeled (left) and observed (center) percent of days with MDA8 ozone exceeding 70 ppb at any monitor within**
 383 **the Los Angeles nonattainment area during May-Sep on weekends and weekdays for 5-year rolling periods between 2002-**
 384 **2019; Observed and modeled trends in May-Sep $\Delta O_{3,DOW,\%>70}$ at Los Angeles area monitors for 5-year rolling periods**
 385 **between 2002-2019 (right). P-values denoted by symbols in the right-hand panel refer to the t-test results comparing mean**
 386 **weekend and weekday values for each 5-year period.**
 387

388 3.2.2 “Disappearing weekday effect” case study

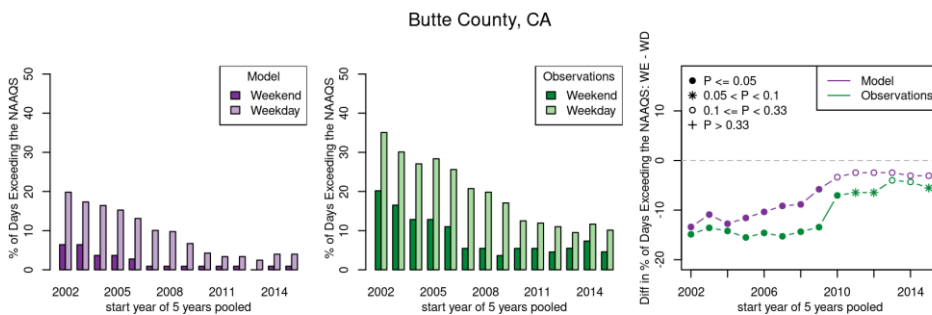
389
 390 The disappearing weekday effect trend type in the $\Delta \overline{O_{3,DOW}}$ metric is evident in 1216 out of the 51
 391 nonattainment areas using observed data and 112 with P-Values < 0.05, 1 with a P-Value between 0.05 and 0.1 and
 392 3 with P-Values between 0.1 and 0.33) and 13 out of the 51 nonattainment areas using modeled data (9 with P-Values
 393 < 0.05, 1 with a P-Value between 0.05 and 0.1 and 3 with P-Values between 0.1 and 0.33) (Figure 4). Of the 51
 394 nonattainment areas analyzed, 21 exhibit this type of trend for the $\Delta O_{3,DOW,\%>70}$ metric based on observed data (12
 395 with P-Values < 0.05, 4 with P-Values between 0.05 and 0.1, and 5 with P-Values between 0.1 and 0.33) and 23 based
 396 on modeled data (17 with P-Values < 0.05, 1 with a P-Value between 0.05 and 0.1 and 5 with P-Values between 0.1
 397 and 0.33) (Figure 5). This trend type is characterized by negative $\Delta \overline{O_{3,DOW}}$ values (i.e., weekday MDA8 ozone higher
 398 than weekend MDA8 ozone) throughout the analysis period indicating NO_x-limited conditions trending upwards
 399 toward zero which appears primarily in rural/agricultural areas in California. The Butte County nonattainment area in
 400 California is one example of an area exhibiting this type of day-of-week trend pattern as is evident using both $\Delta \overline{O_{3,DOW}}$
 401 and $\Delta O_{3,DOW,\%>70}$ (Figures 3 and 9 respectively). The disappearing weekday effect could indicate that sources without
 402 day-of-week activity patterns are becoming more dominant contributors to local NO_x emissions. In that case, the day-
 403 of-week patterns for ambient NO_x concentrations are becoming less pronounced which would result in reductions in
 404 day-of-week MDA8 ozone patterns. An alternate explanation is that local NO_x emissions in general have decreased
 405 substantially enough that local ozone formation has become less important in such areas and a larger fraction of total
 406 ozone is being transported from upwind sources. In that case, the origin of the transported ozone could be a mixture
 407 of multiple source areas that are at varying distances upwind which could lead to a loss in the day-of-week ozone
 408 signal. More analysis would be needed to investigate this idea hypothesis with respect to nonattainment areas of
 409 interest. To our knowledge this trend type has not previously been reported in the literature although we note some
 410 previous national assessments (i.e., Jaffe et al., 2022) did not include many of the smaller rural and agricultural areas
 411 in California where this trend is most prevalent.

412



413

414



415

416

417

418

419

420

421

Figure 9. Modeled (left) and observed (center) percent of days with MDA8 ozone exceeding 70 ppb at any monitor within the Butte County, CA nonattainment area during May-Sep on weekends and weekdays for 5-year rolling periods between 2002-2019; Observed and modeled trends in May-Sep $\Delta O_{3,DOW,\%>70}$ at Butte County, CA area monitors for 5-year rolling periods between 2002-2019 (right). P-values denoted by symbols in the right-hand panel refer to the t-test results comparing mean weekend and weekday values for each 5-year period.

422

3.2.3 “No trend” case studies

423

424

425

426

427

428

429

430

431

432

433

434

Out of the 51 nonattainment areas analyzed, 25 do not have a statistically significant $\Delta \overline{O_{3,DOW}}$ and 6 show no trend based on a p-value cut-off of 0.05 in the $\Delta \overline{O_{3,DOW}}$ metric using observed data and 18 do not have a statistically significant modeled data respectively. Similarly, 12 and 9 show no trend in $\Delta O_{3,DOW,\%>70}$ using observed and modeled data respectively. The reason for the lack of trends may vary by area. Plots for several areas are provided in the supplemental information. Figures S-430, S-834 and S-1137 provide the analysis for New York City which shows no trend for the $\Delta \overline{O_{3,DOW}}$ using observations but a statistically significant disappearing weekend effect transitioning chemical regime trend for this metric using modeled data. Neither Both the model nor and the observations show a significant slight increasing trend in $\Delta O_{3,DOW,\%>70}$. One possible explanation for the lack of trends in New York is the complex nature of the emissions sources and the meteorology impacting ozone formation in this area. Figure S-834 shows $\Delta \overline{O_{3,DOW}}$ trends at three monitors in the New York City nonattainment area occurring in very different locations. The Bronx IS 52 monitor, which is located in an urbanized part of the nonattainment area, shows significant

435 ~~disappearing weekend effect~~ **transitioning chemical regime**, in both modeled and observed $\Delta\overline{O_{3,DOW}}$. In contrast the
436 Long Island – Riverhead monitor and the Bridgeport CT monitor are both located in portions of the nonattainment
437 area that are typically downwind of the urban core on high ozone days and are impacted by complex meteorology
438 associated with the land-water interface near the Long Island sound. The modeled and observed data do not show
439 ~~significant~~ **substantial** $\Delta\overline{O_{3,DOW}}$ trends at the Long Island site and only the model shows ~~disappearing weekend~~
440 ~~effects~~ **transitioning chemical regime** trends at the CT site. Due to the complex nature of this large urban area, some
441 sites may not show trends at all and trends at other sites may be masked when aggregating data across a large number
442 of sites.

Formatted: English (United States)

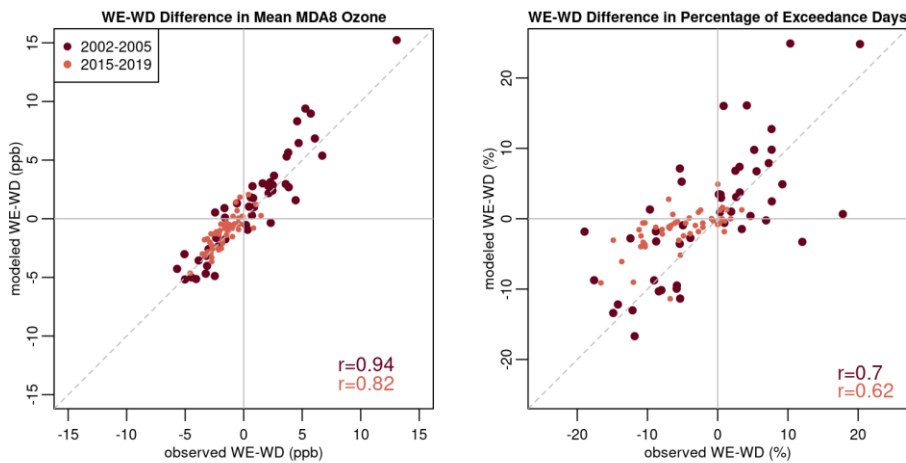
443
444 Several nonattainment areas appear to have negative slopes in $\Delta\overline{O_{3,DOW}}$ at the beginning of the analysis period and
445 positive slopes at the end of the analysis period resulting in no overall trend ~~taken~~ over the entire period. Cincinnati,
446 OH-KY exemplifies this pattern and on closer inspection the patterns appear to mirror annual changes in WE-WD
447 patterns in multiple meteorological parameters (Figure S-1238). For Cincinnati the correlation coefficients between
448 WE-WD MDA8 O₃ differences and WE-WD meteorological parameter differences were 0.77, -0.83, 0.79, 0.89, -0.94,
449 and -0.73 for daily maximum temperature, daily average relative humidity, daily maximum planetary boundary layer
450 height, solar radiation, percent cloud cover and 24-hour transport direction respectively. Other areas exhibiting this
451 behavior are all located in relatively close proximity to Cincinnati, including Louisville, KY-IN and St. Louis, MO-
452 IL and to a lesser extent Columbus, OH and Atlanta, GA. These findings suggest that for these areas even five-year
453 processing blocks may not be sufficient to remove the effects of spurious weekly meteorological variations on ozone.
454 Figure S-1339 shows that the correlation between WE-WD differences in seven meteorological variables and observed
455 $\Delta\overline{O_{3,DOW}}$ do not appear to be a driving factor in significant $\Delta\overline{O_{3,DOW}}$ trends in other areas but it is possible that some
456 additional areas which do not have ~~statistically significant~~ trends in $\Delta\overline{O_{3,DOW}}$ may also be impacted by meteorological
457 variations.

Formatted: English (United States)

459 3.3 Comparison of modeled and observed trends in ozone day-of-week patterns

460
461 The modeled and observed trends in WE-WD differences for each of the 51 nonattainment areas are provided in
462 supplemental tables S1 ($\Delta\overline{O_{3,DOW}}$) and S2 ($\Delta O_{3,DOW,\%>70}$). Figure 10 provides a comparison of modeled to observed
463 WE-WD differences across the 51 nonattainment areas at the beginning of the analysis period (2002-2006) and at the
464 end of the analysis period (2015-2019). Each point represents the WE-WD MDA8 ozone difference for a single
465 nonattainment area, with the left-hand panel showing $\Delta\overline{O_{3,DOW}}$ and the right-hand panel showing $\Delta O_{3,DOW,\%>70}$. Data
466 points falling in the upper right quadrant of each panel represent areas for which both the observations and the modeled
467 DOW patterns suggest NO_x-saturated conditions. Data points in the lower left quadrant of each panel represent areas
468 for which both the observations and the model DOW patterns suggest NO_x-limited conditions. In the earlier 2002-
469 2006 time-period, there are a large number of areas falling in both the upper right and lower left quadrants for both
470 metrics. In the 2015-2019 time-period, almost all areas are located in the lower left quadrant for both metrics
471 suggesting that most US nonattainment areas have transitioned into NO_x-limited conditions. The correlation of

472 modeled and observed WE-WD differences is quite high ($r = 0.94$ and 0.82 for $\overline{\Delta O_{3,DOW}}$ in the earliest and most recent
 473 time periods, respectively, and $r = 0.7$ and 0.62 for $\Delta O_{3,DOW,\%>70}$ in the earliest and most recent time periods,
 474 respectively). For both metrics, the majority of points fall above the 1:1 line indicating that, in general, the model
 475 overestimated the degree of NO_x -saturated conditions and underestimated the degree of NO_x -limited conditions.
 476

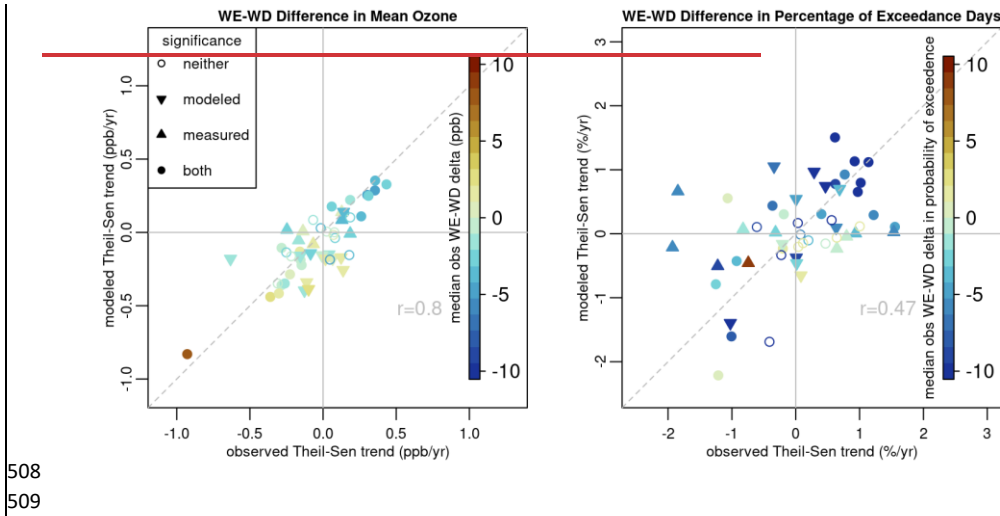


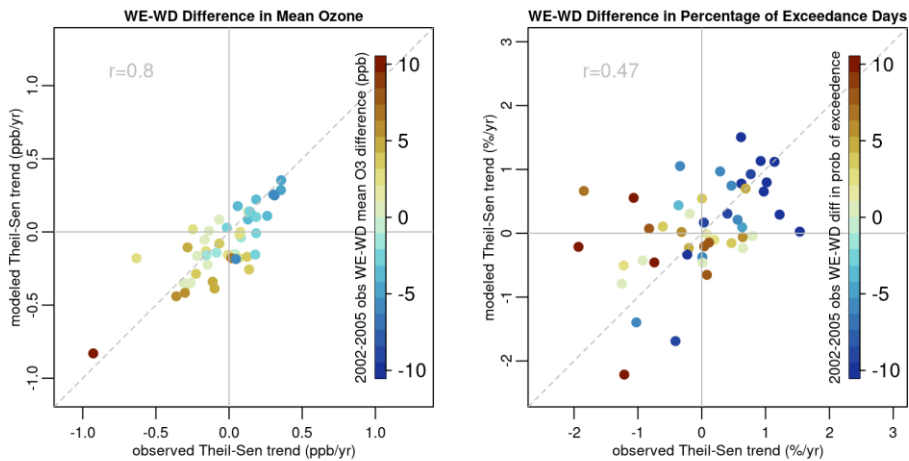
477
 478 **Figure 10. Comparison of modeled and observed WE-WD MDA8 O₃ differences for $\overline{\Delta O_{3,DOW}}$ (left panel) and $\Delta O_{3,DOW,\%>70}$**
 479 **(right panel). Differences shown for the 2002-2006 time period and for the 2015-2019 time period. Each dot represents a**
 480 **different nonattainment area.**

481
 482 Maps in Figures 4 and 5 show the locations of areas predicted to have ~~disappearing weekend effect~~ **transitioning**
 483 **chemical regime** trends, disappearing weekday effect trends and no trends for $\overline{\Delta O_{3,DOW}}$ and $\Delta O_{3,DOW,\%>70}$
 484 respectively. The maps show general consistency among which areas are predicted to have each trend type between
 485 observations and the model, ~~although some areas predicted to have significant trends with one dataset or with one~~
 486 ~~metric do not have significant trends with the other dataset or metric.~~ Nine areas are predicted to have ~~disappearing~~
 487 ~~weekend effect trend~~ **transitioning chemical regime trends with P-Values < 0.05** in both datasets and with both metrics
 488 indicating strong agreement that they are shifting to more NO_x -limited conditions: Milwaukee, WI; Houston, TX;
 489 Phoenix, AZ; Denver, CO; Northern Wasatch Front, UT; Southern Wasatch Front, UT; Las Vegas, NV; Los Angeles
 490 – San Bernardino County, CA; Los Angeles – South Coast, CA; and San Diego, CA.

491
 492 Figure 11 compares modeled and observed ~~Theil~~ **Theil**-Sen slopes in WE-WD MDA8 O₃ differences across all areas.
 493 Each point represents a single nonattainment area color-coded by ~~median 2002-2005~~ $\overline{\Delta O_{3,DOW}}$ or $\Delta O_{3,DOW,\%>70}$. The
 494 correlation of modeled versus observed ~~Theil~~ **Theil**-Sen slopes using $\overline{\Delta O_{3,DOW}}$ is stronger ($r = 0.8$) than the correlation
 495 using $\Delta O_{3,DOW,\%>70}$ ($r = 0.47$). While the model does not always correctly predict the ~~Theil~~ **Theil**-Sen slope, the data
 496 falls close to the 1:1 line for the $\overline{\Delta O_{3,DOW}}$ suggesting that the model does not systematically over or under predict the

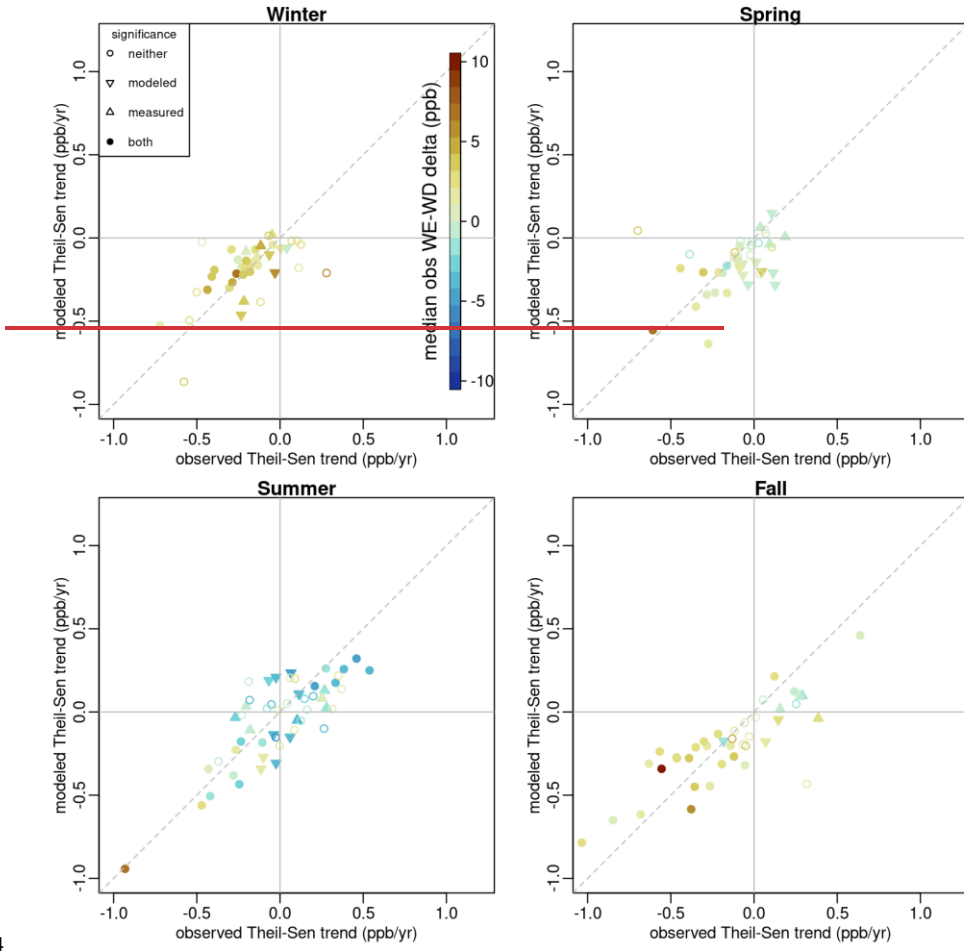
497 trends in WE-WD differences from 2002-2019. The trend types described above for $\overline{\Delta O_{3,DOW}}$ metric are visible in the
 498 left-panel of Figure 11. Most NO_x -saturated areas (yellow and brown symbols) and some NO_x -limited areas (blue
 499 symbols) have negative Theil-Sen slopes (i.e. transitioning chemical regime) towards NO_x -limited conditions
 500 similar to those described above for Denver and Los Angeles (shown as the dark brown symbol at the bottom-left of
 501 the plot). Areas with positive Theil-Sen slopes tend to be the most NO_x -limited areas (darker blue symbols) and
 502 represent the disappearing weekday trends demonstrated by Butte County. The model is not as accurate at predicting
 503 $\Delta O_{3,DOW, \%>70}$ Theil-Sen slopes as $\overline{\Delta O_{3,DOW}}$ Theil-Sen slopes, as evidenced by the increased scatter in the right-
 504 hand panel of Figure 11 compared to the left-hand panel. Some areas have few exceedances of the NAAQS in the
 505 later years of the trends period and this small sample size could explain the difference between the monitored and
 506 modeled slopes, given that the model predicted fewer exceedance days than were observed in many areas.
 507



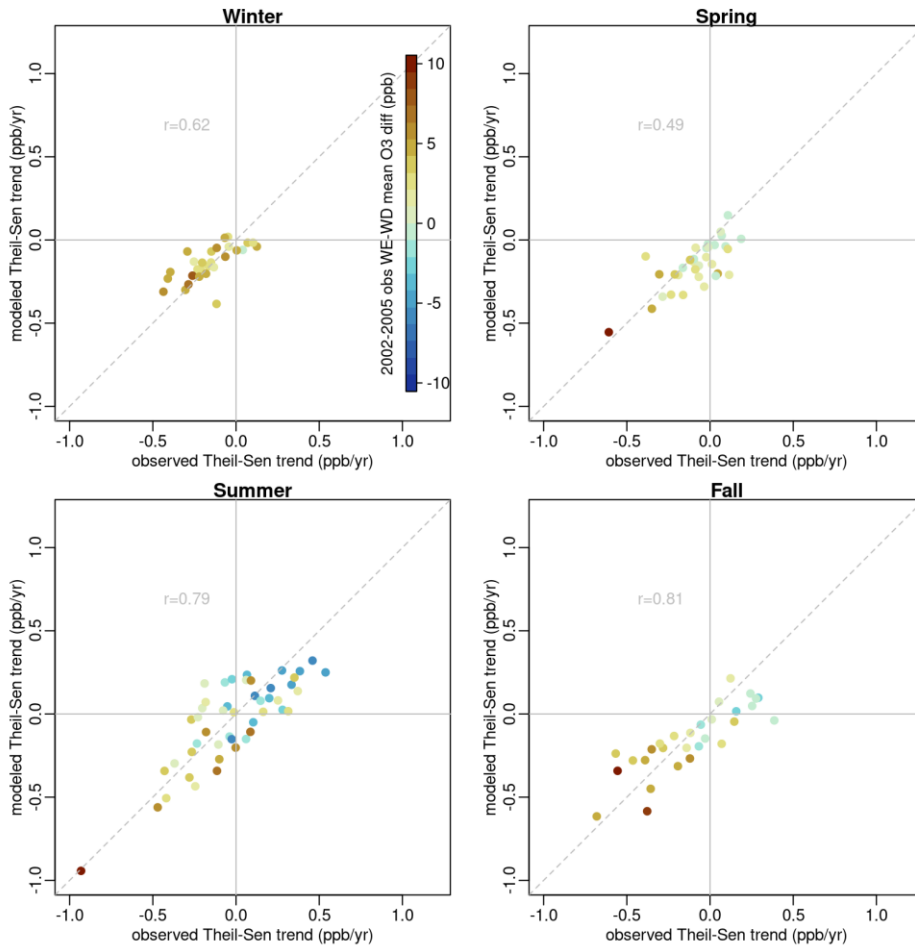


510
 511 **Figure 11. Comparison of modeled and observed Theil-Sen slopes in May-Sep WE-WD MDA8 O₃ differences across**
 512 **all nonattainment areas for $\Delta\overline{O_{3,DOW}}$ (left panel) and $\Delta O_{3,DOW,\%>70}$ (right panel). Whether or not the trend is significant**
 513 **with observed and/or modeled data is indicated by the shape of the symbol. Median WE-WD differences across all years for**
 514 **the 2002-2005 time-period are indicated by the color scalebar with positive differences (NO_x-saturated areas) shown in**
 515 **shades of yellow and brown and negative differences (NO_x-limited areas) shown in shades of blue. Note that the brown**
 516 **symbol ~~on~~at the bottom-left of both figurespanels represents the Los Angeles nonattainment area.**
 517

518 Figure 12 shows the comparison of $\overline{\Delta O_{3,DOW}}$ Theil-Sen slopes by season. The summer plot looks similar
 519 to the May-September plot shown in Figure 11. Winter, spring, and fall data show median $\overline{\Delta O_{3,DOW}}$ near zero or
 520 greater than zero in most nonattainment areas suggesting transitional or NO_x-saturated conditions in these seasons.
 521 Both observations and model predictions suggest $\overline{\Delta O_{3,DOW}}$ negative Theil-Sen slopes in these seasons suggesting
 522 that nonattainment areas in the US may be transitioning towards NO_x-limited conditions even outside of the summer
 523 ozone season.



524
525



526
 527 **Figure 12. Comparison of modeled and observed $\Delta O_{3,DOW}$ Theil-Sen slopes across all nonattainment areas in**
 528 **winter (top left), spring (top right), summer (bottom left) and fall (bottom right). Whether or not the trend is significant**
 529 **with observed and/or modeled data is indicated by the shape of the symbol. Median WE-WD differences across all years for**
 530 **the 2002-2005 time period are indicated by the color scale with positive differences (NO_x-saturated areas) shown in**
 531 **shades of yellow and brown and negative differences (NO_x-limited areas) shown in shades of blue. Note that year-round**
 532 **ozone monitoring is not required in some parts of the US and therefore monitoring data may not be available outside the**
 533 **May-September period in some areas.**

Formatted: English (Canada)

534 **4 Conclusions**

535
 536 While this assessment has provided insight into the ozone formation regimes across high-ozone locations in the US,
 537 some key questions remain about the important drivers for year-to-year changes in DOW MDA8 ozone patterns and
 538 which of those drivers are well captured by the EQUATES dataset. First, while NO_x and VOC emissions have been

539 steadily decreasing across most areas of the US, exceptions to that pattern include increasing wildfire emissions
540 especially in the Western US and increasing emissions from oil and gas activities near US nonattainment areas in
541 Texas, Colorado, New Mexico and Utah. Future work could focus on areas impacted by these two emissions sources
542 to assess both the impact of these increasing emissions on ozone formation regimes and the ability of the EQUATES
543 dataset to capture those impacts. Second, this assessment predominantly focused on [MDA8](#) ozone values across the
544 May-Sep ozone season, however, past work has identified some seasonally varying ozone biases within the CMAQ
545 model (Appel et al., 2021). Specifically, EQUATES has a tendency to underpredict ozone during the spring and
546 overpredict ozone later in the summer (Figures [S-4440](#) and [S-1541](#)). Given that ozone formation tends to be more
547 NO_x-saturated in the springtime than in the summer (Jin et al., 2020; Jin et al., 2017), a more in-depth assessment
548 would be needed to fully characterize the extent that differences in observed and modeled WE-WD [MDA8](#) ozone
549 differences are impacted by this seasonally varying model performance. Third, we assessed DOW [MDA8](#) ozone
550 patterns across multiple complex urban areas that encompassed spatially heterogeneous emissions sources and
551 meteorology. For some of these areas (e.g. Los Angeles, CA and Denver, CO) the sign of the [ThielTheil](#)-Sen slopes
552 in WE-WD [MDA8](#) ozone appeared consistent across monitoring locations while in others (e.g. New York City, NY)
553 different monitoring locations across the area appeared to show different types of trends. Further local scale
554 investigation into each of these areas would be necessary to fully characterize the nuances of DOW and year-to-year
555 variations in emission and meteorology that obscure the [MDA8](#) ozone DOW trends in some areas but not others when
556 aggregating across monitor locations in those areas. Finally, an intriguing trend in [MDA8](#) ozone DOW patterns was
557 identified in multiple rural and agricultural areas of California. Recent literature has suggested that soil NO emissions,
558 which are unlikely to have a DOW emissions pattern, are an important NO_x emissions source in agricultural locations
559 of California (Almaraz et al., 2018; Zhu et al., 2023). Could the [MDA8](#) ozone DOW trends observed in these areas be
560 reflective of the increasing relative importance of NO_x sources other than mobile sources in those locations? More
561 assessment is needed to definitively determine whether the trend in a decreasing weekday effect is a reliable indicator
562 of areas that are becoming more dominated by local NO_x sources that do not vary by DOW, more dominated by
563 transported ozone, or some other factor. It is important to note that transported ozone may come from nearby regional
564 sources or from longer range sources provided the transport times are sufficient to mask any DOW patterns that would
565 be evident in the source region.

566
567 In this analysis we found that trends in ozone formation chemistry may not always be clearly shown by trends in DOW
568 patterns which are impacted by a complex set of local factors including meteorology, the mix of local emissions
569 sources and monitor locations in relationship to land-water interfaces. Lack of trends appear more often using observed
570 data than modeled data (Figures 4 and 5) meaning that, while the model accurately captures [ThielTheil](#)-Sen slopes for
571 $\Delta O_{3,DOW}$ and $\Delta O_{3,DOW,\%>70}$ (Figure 11), [lower P-values below 0.05](#) are less common using observational data. This
572 suggests that there may be some stochastic processes making observed year-to-year WE-WD [MDA8](#) ozone differences
573 noisy which are not fully captured by the model. Even with these limitations, this analysis has shown that DOW
574 patterns in ambient NO_x concentrations persist in US urban areas but have become less prominent [in some areas while](#)
575 [others have transitioned from positive WE-WD MDA8 ozone differences to negative WE-WD MDA8 ozone](#)

576 [differences](#) over the 18-year period analyzed. These DOW NO_x differences have resulted in distinctive DOW [MDA8](#)
577 ozone patterns in many of the nonattainment areas assessed. The EQUATES modeling simulations appear to show
578 larger and more positive WE-WD [MDA8](#) ozone differences than observational data suggesting that ozone formation
579 in this modeling dataset is less NO_x-limited than in the observations. Despite this discrepancy, the EQUATES dataset
580 captures year-to-year changes in WE-WD [MDA8](#) ozone patterns as demonstrated by high correlation of the
581 ~~ThielTheil~~-Sen slopes for WE-WD [MDA8](#) ozone differences. ~~Both the WE-WD ozone trends and The~~ agreement
582 between the modeled and observation datasets are more apparent when assessing summertime mean MDA8 ozone
583 than when analyzing extreme values using the percentage of exceedance days metric. Assessing frequencies or
584 magnitudes of extreme values is challenging using a dataset with a limited number of weekend and weekday days due
585 to the stochastic and infrequent nature of high ozone events in many areas.

586
587 While there are multiple types of measurements and modeling assessments that can be applied to characterize local
588 ozone formation regimes, many of these require specialized measurements or datasets that are not readily available in
589 all areas. In contrast, assessing DOW [MDA8](#) ozone patterns requires only routine daily ozone measurements that are
590 widely available across urban areas in the US and in other countries. Consequently, this type of assessment is a useful
591 tool and may be applied in many areas using routine measurements. In locations with long-term measurements, DOW
592 patterns offer a method to look at trends in ozone formation chemistry over time. While DOW patterns in [MDA8](#)
593 ozone are especially useful given the wide availability of data required for this type of assessment, we anticipate that
594 in the near future additional datasets for assessing ozone chemical formation regimes will become more widely
595 available. Specifically, O₃, NO₂ and HCHO data from the recently launched TEMPO satellite may provide the ability
596 to better understand the relationships between WE-WD [MDA8](#) ozone patterns and precursor concentrations.

597 **Author contributions**

598 All authors contributed to conceptualization of the project. HS, CH, KF, BW, and WA contributed to data curation.
599 HS conducted formal analysis. HS, CH, AW, KF, BW, BH, and SK contributed to developing the methodology.
600 HS and BW developed software for performing the analysis. HS, CH, AW, JL, NP, BW, and GT contributed to
601 validation. HS, BW, and BH helped visualize the data. All authors contributed to the writing and editing of the
602 manuscript.

603 **Competing interests**

604 The authors declare that they have no conflict of interest.

605

606 **[Data accessibility statement](#)**

607 [The observed and CMAQ estimated gas species data and meteorological data that were used in the analysis are](#)
608 [available at https://doi.org/10.5281/zenodo.10222897.](https://doi.org/10.5281/zenodo.10222897)

609 **Disclaimer:** The views expressed in this manuscript are those of the authors and do not necessarily reflect the views
610 or policies of the U.S. Environmental Protection Agency.

611 **Acknowledgements**

612 The authors would like to acknowledge Chris Nolte and Golam Sarwar for helpful comments on this manuscript. [We](#)
613 [thank Daniel Jaffe, David Parish, and the anonymous reviewer for their helpful comments through ACP's open](#)
614 [discussion review.](#)

615 **References**

616 Adame, J. A., Hernández-Ceballos, M. Á., Sorribas, M., Lozano, A., and Morena, B. A. D. I.: Weekend-
617 Weekday Effect Assessment for O₃, NO_x, CO and PM₁₀ in Andalusia, Spain (2003-2008), *Aerosol and Air*
618 *Quality Research*, 14, 1862-1874, 10.4209/aaqr.2014.02.0026, 2014.

619 Almaraz, M., Bai, E., Wang, C., Trousdell, J., Conley, S., Faloona, I., and Houlton, B. Z.: Agriculture is a
620 major source of NO_x pollution in California, *Science Advances*, 4, eaao3477,
621 doi:10.1126/sciadv.aao3477, 2018.

622 Appel, K. W., Bash, J. O., Fahey, K. M., Foley, K. M., Gilliam, R. C., Hogrefe, C., Hutzell, W. T., Kang, D.,
623 Mathur, R., Murphy, B. N., Napelenok, S. L., Nolte, C. G., Pleim, J. E., Pouliot, G. A., Pye, H. O. T., Ran, L.,
624 Roselle, S. J., Sarwar, G., Schwede, D. B., Sidi, F. I., Spero, T. L., and Wong, D. C.: The Community
625 Multiscale Air Quality (CMAQ) model versions 5.3 and 5.3.1: system updates and evaluation, *Geosci.*
626 *Model Dev.*, 14, 2867-2897, 10.5194/gmd-14-2867-2021, 2021.

627 Atkinson-Palombo, C. M., Miller, J. A., and Balling, R. C.: Quantifying the ozone "weekend effect" at
628 various locations in Phoenix, Arizona, *Atmospheric Environment*, 40, 7644-7658,
629 <https://doi.org/10.1016/j.atmosenv.2006.05.023>, 2006.

630 Blanchard, C. L. and Tanenbaum, S.: Weekday/Weekend Differences in Ambient Air Pollutant
631 Concentrations in Atlanta and the Southeastern United States, *Journal of the Air & Waste Management*
632 *Association*, 56, 271-284, 10.1080/10473289.2006.10464455, 2006.

633 Blanchard, C. L., Tanenbaum, S., and Lawson, D. R.: Differences between Weekday and Weekend Air
634 Pollutant Levels in Atlanta; Baltimore; Chicago; Dallas-Fort Worth; Denver; Houston; New York; Phoenix;
635 Washington, DC; and Surrounding Areas, *Journal of the Air & Waste Management Association*, 58, 1598-
636 1615, 10.3155/1047-3289.58.12.1598, 2008.

637 Bruntz, S. M., Cleveland, W. S., Graedel, T. E., Kleiner, B., and Warner, J. L.: OZONE CONCENTRATIONS IN
638 NEW-JERSEY AND NEW-YORK - STATISTICAL ASSOCIATION WITH RELATED VARIABLES, *Science*, 186, 257-
639 259, 10.1126/science.186.4160.257, 1974.

640 Chinkin, L. R., Coe, D. L., Funk, T. H., Hafner, H. R., Roberts, P. T., Ryan, P. A., and Lawson, D. R.: Weekday
641 versus Weekend Activity Patterns for Ozone Precursor Emissions in California's South Coast Air Basin,
642 *Journal of the Air & Waste Management Association*, 53, 829-843, 10.1080/10473289.2003.10466223,
643 2003.

644 Cleveland, W. S., Graedel, T. E., Kleiner, B., and Warner, J. L.: SUNDAY AND WORKDAY VARIATIONS IN
645 PHOTOCHEMICAL AIR-POLLUTANTS IN NEW-JERSEY AND NEW-YORK, *Science*, 186, 1037-1038,
646 10.1126/science.186.4168.1037, 1974.

647 de Foy, B., Brune, W. H., and Schauer, J. J.: Changes in ozone photochemical regime in Fresno, California
648 from 1994 to 2018 deduced from changes in the weekend effect, *Environmental Pollution*, 263, 114380,
649 <https://doi.org/10.1016/j.envpol.2020.114380>, 2020.

650 EPA, U.: EQUATESv1.0: Emissions, WRF/MCIP, CMAQv5.3.2 Data -- 2002-2019 US_12km and
651 NHEMI_108km (V5), UNC Dataverse [dataset], doi:10.15139/S3/F2KJSK, 2021.

652 Fisher, R. A.: The Logic of Inductive Inference, *Journal of the Royal Statistical Society*, 98, 39-82,
653 10.2307/2342435, 1935.

654 Foley, K. M., Pouliot, G. A., Eyth, A., Aldridge, M. F., Allen, C., Appel, K. W., Bash, J. O., Beardsley, M.,
655 Beidler, J., Choi, D., Farkas, C., Gilliam, R. C., Godfrey, J., Henderson, B. H., Hogrefe, C., Koplitz, S. N.,
656 Mason, R., Mathur, R., Misenis, C., Possiel, N., Pye, H. O. T., Reynolds, L., Roark, M., Roberts, S.,

657 Schwede, D. B., Seltzer, K. M., Sonntag, D., Talgo, K., Toro, C., Vukovich, J., Xing, J., and Adams, E.: 2002–
658 2017 anthropogenic emissions data for air quality modeling over the United States, Data in Brief, 47,
659 109022, <https://doi.org/10.1016/j.dib.2023.109022>, 2023.

660 Fujita, E. M., Stockwell, W. R., Campbell, D. E., Keislar, R. E., and Lawson, D. R.: Evolution of the
661 Magnitude and Spatial Extent of the Weekend Ozone Effect in California’s South Coast Air Basin, 1981–
662 2000, Journal of the Air & Waste Management Association, 53, 802-815,
663 10.1080/10473289.2003.10466225, 2003a.

664 Fujita, E. M., Campbell, D. E., Zielinska, B., Sagebiel, J. C., Bowen, J. L., Goliff, W. S., Stockwell, W. R., and
665 Lawson, D. R.: Diurnal and Weekday Variations in the Source Contributions of Ozone Precursors in
666 California’s South Coast Air Basin, Journal of the Air & Waste Management Association, 53, 844-863,
667 10.1080/10473289.2003.10466226, 2003b.

668 Gao, H. O.: Day of week effects on diurnal ozone/NOx cycles and transportation emissions in Southern
669 California, Transportation Research Part D: Transport and Environment, 12, 292-305,
670 <https://doi.org/10.1016/j.trd.2007.03.004>, 2007.

671 Gao, H. O. and Niemeier, D. A.: The impact of rush hour traffic and mix on the ozone weekend effect in
672 southern California, Transportation Research Part D: Transport and Environment, 12, 83-98,
673 <https://doi.org/10.1016/j.trd.2006.12.001>, 2007.

674 Jaffe, D. A., Ninneman, M., and Chan, H. C.: NOx and O3 Trends at U.S. Non-Attainment Areas for 1995–
675 2020: Influence of COVID-19 Reductions and Wildland Fires on Policy-Relevant Concentrations, 127,
676 e2021JD036385, <https://doi.org/10.1029/2021JD036385>, 2022.

677 Jiménez, P., Parra, R., Gassó, S., and Baldasano, J. M.: Modeling the ozone weekend effect in very
678 complex terrains: a case study in the Northeastern Iberian Peninsula, Atmospheric Environment, 39,
679 429-444, <https://doi.org/10.1016/j.atmosenv.2004.09.065>, 2005.

680 Jin, X., Fiore, A., Boersma, K. F., Smedt, I. D., and Valin, L.: Inferring Changes in Summertime Surface
681 Ozone–NOx–VOC Chemistry over U.S. Urban Areas from Two Decades of Satellite and Ground-Based
682 Observations, Environmental Science & Technology, 54, 6518-6529, 10.1021/acs.est.9b07785, 2020.

683 Jin, X., Fiore, A. M., Murray, L. T., Valin, L. C., Lamsal, L. N., Duncan, B., Folkert Boersma, K., De Smedt, I.,
684 Abad, G. G., Chance, K., and Tonnesen, G. S.: Evaluating a Space-Based Indicator of Surface Ozone-NOx-
685 VOC Sensitivity Over Midlatitude Source Regions and Application to Decadal Trends, Journal of
686 Geophysical Research: Atmospheres, 122, 10,439-410,461, <https://doi.org/10.1002/2017JD026720>,
687 2017.

688 Kendall, M. G.: Rank Correlation Methods, 4th edition, Charles Griffin, London1975.

689 Koo, B., Jung, J., Pollack, A. K., Lindhjem, C., Jimenez, M., and Yarwood, G.: Impact of meteorology and
690 anthropogenic emissions on the local and regional ozone weekend effect in Midwestern US,
691 Atmospheric Environment, 57, 13-21, <https://doi.org/10.1016/j.atmosenv.2012.04.043>, 2012.

692 Kopplitz, S., Simon, H., Henderson, B., Liljegren, J., Tonnesen, G., Whitehill, A., and Wells, B.: Changes in
693 Ozone Chemical Sensitivity in the United States from 2007 to 2016, ACS Environmental Au, 2, 206-222,
694 10.1021/acsenvironau.1c00029, 2022.

695 Krotkov, N. A., McLinden, C. A., Li, C., Lamsal, L. N., Celarier, E. A., Marchenko, S. V., Swartz, W. H.,
696 Bucsela, E. J., Joiner, J., Duncan, B. N., Boersma, K. F., Veefkind, J. P., Levelt, P. F., Fioletov, V. E.,
697 Dickerson, R. R., He, H., Lu, Z. F., and Streets, D. G.: Aura OMI observations of regional SO2 and NO2
698 pollution changes from 2005 to 2015, Atmospheric Chemistry and Physics, 16, 4605-4629, 10.5194/acp-
699 16-4605-2016, 2016.

700 Lamsal, L. N., Duncan, B. N., Yoshida, Y., Krotkov, N. A., Pickering, K. E., Streets, D. G., and Lu, Z. F.: U.S.
701 NO2 trends (2005-2013): EPA Air Quality System (AQS) data versus improved observations from the
702 Ozone Monitoring Instrument (OMI), Atmospheric Environment, 110, 130-143,
703 10.1016/j.atmosenv.2015.03.055, 2015.

704 Mann, H. B.: Nonparametric Tests Against Trend, Econometrica, 13, 245-259, 10.2307/1907187, 1945.

705 Marr, L. C. and Harley, R. A.: Spectral analysis of weekday-weekend differences in ambient ozone,
706 nitrogen oxide, and non-methane hydrocarbon time series in California, *Atmospheric Environment*, 36,
707 2327-2335, 10.1016/s1352-2310(02)00188-7, 2002a.

708 Marr, L. C. and Harley, R. A.: Modeling the effect of weekday-weekend differences in motor vehicle
709 emissions on photochemical air pollution in central California, *Environmental Science & Technology*, 36,
710 4099-4106, 10.1021/es020629x, 2002b.

711 Martins, E. M., Nunes, A. C. L., and Correa, S. M.: Understanding Ozone Concentrations During
712 Weekdays and Weekends in the Urban Area of the City of Rio de Janeiro, *Journal of the Brazilian
713 Chemical Society*, 26, 1967-1975, 10.5935/0103-5053.20150175, 2015.

714 Mehta, C. R. and Patel, N. R.: A Network Algorithm for Performing Fisher's Exact Test in $r \times c$ Contingency
715 Tables, *Journal of the American Statistical Association*, 78, 427-434, 10.2307/2288652, 1983.

716 Murphy, J. G., Day, D. A., Cleary, P. A., Wooldridge, P. J., Millet, D. B., Goldstein, A. H., and Cohen, R. C.:
717 The weekend effect within and downwind of Sacramento – Part 1: Observations of ozone,
718 nitrogen oxides, and VOC reactivity, *Atmos. Chem. Phys.*, 7, 5327-5339, 10.5194/acp-7-5327-2007, 2007.

719 Paschalidou, A. K. and Kassomenos, P. A.: Comparison of Air Pollutant Concentrations between
720 Weekdays and Weekends in Athens, Greece for Various Meteorological Conditions, *Environmental
721 Technology*, 25, 1241-1255, 10.1080/09593332508618372, 2004.

722 Pierce, T., Hogrefe, C., Trivikrama Rao, S., Porter, P. S., and Ku, J.-Y.: Dynamic evaluation of a regional air
723 quality model: Assessing the emissions-induced weekly ozone cycle, *Atmospheric Environment*, 44,
724 3583-3596, <https://doi.org/10.1016/j.atmosenv.2010.05.046>, 2010.

725 Pires, J. C. M.: Ozone Weekend Effect Analysis in Three European Urban Areas, *CLEAN – Soil, Air, Water*,
726 40, 790-797, <https://doi.org/10.1002/clen.201100410>, 2012.

727 Plocoste, T., Dorville, J.-F., Monjoly, S., Jacoby-Koaly, S., and André, M.: Assessment of nitrogen oxides
728 and ground-level ozone behavior in a dense air quality station network: Case study in the Lesser Antilles
729 Arc, *Journal of the Air & Waste Management Association*, 68, 1278-1300,
730 10.1080/10962247.2018.1471428, 2018.

731 Pun, B. K., Seigneur, C., and White, W.: Day-of-Week Behavior of Atmospheric Ozone in Three U.S. Cities,
732 *Journal of the Air & Waste Management Association*, 53, 789-801, 10.1080/10473289.2003.10466231,
733 2003.

734 Roberts, S. J., Salawitch, R. J., Wolfe, G. M., Marvin, M. R., Canty, T. P., Allen, D. J., Hall-Quinlan, D. L.,
735 Krask, D. J., and Dickerson, R. R.: Multidecadal trends in ozone chemistry in the Baltimore-Washington
736 Region, *Atmospheric Environment*, 285, 119239, <https://doi.org/10.1016/j.atmosenv.2022.119239>,
737 2022.

738 Rubio, M. A., Sanchez, K., and Lissi, Y. E.: OZONE LEVELS ASSOCIATED TO THE PHOTOCHEMICAL SMOG IN
739 SANTIAGO OF CHILE. THE ELUSIVE ROL OF HYDROCARBONS, *Journal of the Chilean Chemical Society*, 56,
740 709-711, 2011.

741 Russell, A. R., Valin, L. C., and Cohen, R. C.: Trends in OMI NO₂ observations over the United States:
742 effects of emission control technology and the economic recession, *Atmospheric Chemistry and Physics*,
743 12, 12197-12209, 10.5194/acp-12-12197-2012, 2012.

744 Seinfeld, J. H. and Pandis, S. N.: *Atmospheric chemistry and physics: from air pollution to climate change*,
745 John Wiley & Sons 2016.

746 Sen, P. K.: Estimates of the Regression Coefficient Based on Kendall's Tau, *Journal of the American
747 Statistical Association*, 63, 1379-1389, 10.1080/01621459.1968.10480934, 1968.

748 Sillman, S.: THE USE OF NO_y, H₂O₂, AND HNO₃ AS INDICATORS FOR OZONE-NO_x-HYDROCARBON
749 SENSITIVITY IN URBAN LOCATIONS, *Journal of Geophysical Research-Atmospheres*, 100, 14175-14188,
750 10.1029/94jd02953, 1995.

751 Sillman, S.: The relation between ozone, NO_x and hydrocarbons in urban and polluted rural
752 environments, *Atmospheric Environment*, 33, 1821-1845, 10.1016/s1352-2310(98)00345-8, 1999.

753 Sillman, S., Logan, J. A., and Wofsy, S. C.: THE SENSITIVITY OF OZONE TO NITROGEN-OXIDES AND
754 HYDROCARBONS IN REGIONAL OZONE EPISODES, *Journal of Geophysical Research-Atmospheres*, 95,
755 1837-1851, 10.1029/JD095iD02p01837, 1990.
756 Simon, H., Reff, A., Wells, B., Xing, J., and Frank, N.: Ozone Trends Across the United States over a Period
757 of Decreasing NOx and VOC Emissions, *Environmental Science & Technology*, 49, 186-195,
758 10.1021/es504514z, 2015.
759 Singh, S. and Kavouras, I. G.: Trends of Ground-Level Ozone in New York City Area during
760 2007–2017, 13, 114, 2022.
761 Theil, H.: A Rank-Invariant Method of Linear and Polynomial Regression Analysis, in: Henri Theil's
762 Contributions to Economics and Econometrics: Econometric Theory and Methodology, edited by: Raj, B.,
763 and Koerts, J., Springer Netherlands, Dordrecht, 345-381, 10.1007/978-94-011-2546-8_20, 1992.
764 Toro, C., Foley, K., Simon, H., Henderson, B., Baker, K. R., Eyth, A., Timin, B., Appel, W., Luecken, D.,
765 Beardsley, M., Sonntag, D., Possiel, N., and Roberts, S.: Evaluation of 15 years of modeled atmospheric
766 oxidized nitrogen compounds across the contiguous United States, *Elementa-Science of the*
767 *Anthropocene*, 9, 10.1525/elementa.2020.00158, 2021.
768 U.S. Environmental Protection Agency: Integrated Science Assessment (ISA) for Particulate Matter (Final
769 report, Dec 2019). U.S. Environmental Protection Agency, Washington, DC, EPA/600/R-19/188, 2019.
770 Warneke, C., de Gouw, J. A., Edwards, P. M., Holloway, J. S., Gilman, J. B., Kuster, W. C., Graus, M., Atlas,
771 E., Blake, D., Gentner, D. R., Goldstein, A. H., Harley, R. A., Alvarez, S., Rappenglueck, B., Trainer, M., and
772 Parrish, D. D.: Photochemical aging of volatile organic compounds in the Los Angeles basin: Weekday-
773 weekend effect, 118, 5018-5028, <https://doi.org/10.1002/jgrd.50423>, 2013.
774 Welch, B. L.: THE GENERALIZATION OF 'STUDENT'S' PROBLEM WHEN SEVERAL DIFFERENT POPULATION
775 VARIANCES ARE INVOLVED, *Biometrika*, 34, 28-35, 10.1093/biomet/34.1-2.28, 1947.
776 Wells, B., Dolwick, P., Eder, B., Evangelista, M., Foley, K., Mannshardt, E., Misenis, C., and Weishampel,
777 A.: Improved estimation of trends in U.S. ozone concentrations adjusted for interannual variability in
778 meteorological conditions, *Atmospheric Environment*, 248, 118234,
779 <https://doi.org/10.1016/j.atmosenv.2021.118234>, 2021.
780 Zhang, G., Sun, Y., Xu, W., Wu, L., Duan, Y., Liang, L., and Li, Y.: Identifying the O3 chemical regime
781 inferred from the weekly pattern of atmospheric O3, CO, NOx, and PM10: Five-year observations at a
782 center urban site in Shanghai, China, *Science of The Total Environment*, 888, 164079,
783 <https://doi.org/10.1016/j.scitotenv.2023.164079>, 2023.
784 Zhu, Q., Place, B., Pfannerstill, E. Y., Tong, S., Zhang, H., Wang, J., Nussbaumer, C. M., Wooldridge, P.,
785 Schulze, B. C., Arata, C., Bucholtz, A., Seinfeld, J. H., Goldstein, A. H., and Cohen, R. C.: Direct
786 observations of NOx emissions over the San Joaquin Valley using airborne flux measurements during
787 RECAP-CA 2021 field campaign, *Atmos. Chem. Phys. Discuss.*, 2023, 1-21, 10.5194/acp-2023-3, 2023.

788
789
790
791
792
793
794
795

796
797
798
799
800
801
802

